



Εθνικό Μετσόβιο Πολυτεχνείο- Σχολή Πολιτικών Μηχανικών
Τομέας Υδατικών Πόρων και Περιβάλλοντος
Technische Universität Berlin - Institut für Bauingenieurwesen
Fachgebiet Wasserwirtschaft und Hydrosystemmodellierung



Διπλωματική Εργασία

Διερεύνηση
Οριακών και Αρχικών Συνθηκών σε
Μοντέλο Διφασικής Ροής για την
Προσομοίωση Ταχείας Διήθησης Νερού
σε Μακροπορώδη Εδάφη

Αφροδίτη Κατερινοπούλου

Βερολίνο, Ιούλιος 2009

Επιβλέποντες Διδάσκοντες:
Dipl.- Ing. Leopold Stadler, Prof. Dipl.- Ing. Reinhard
Hinkelmann, Καθ. Διπλ.- Μηχ. Δημήτρης Κουτσογιάννης



National Technical University of Athens-School of Civil Engineering
Department of Water Resources and Environmental Engineering
Technische Universität Berlin - Institut für Bauingenieurwesen
Fachgebiet Wasserwirtschaft und Hydrosystemmodellierung



Diploma Thesis

Development of Concepts to Generate Boundary and Initial Conditions for a Two-Phase Flow Dual-Permeability Model to Simulate the Rapid Water Infiltration into Macro-Porous Soils

Aphroditi Katerinopoulou

Berlin, July 2009

Supervisors:

Dipl.- Ing. Leopold Stadler, Prof. Dipl.- Ing. Reinhard
Hinkelmann, Prof. Dipl.- Ing. Demetris Koutsoyiannis

Περίληψη

Η παρούσα εργασία έχει ως θέμα τη διερεύνηση των οριακών συνθηκών στην προσομοίωση της διήθησης του νερού στο έδαφος με το πακέτο προσομοίωσης MUFTE-UG. Η μελέτη αυτή εντάσσεται στην εφαρμογή και περαιτέρω ανάπτυξη του λογισμικού MUFTE-UG, στα πλαίσια του προγράμματος Grosshang στη δυτική Αυστρία, που αφορά ολισθαίνουσες πλαγιές.

Κατ' αρχάς γίνεται μια γενική περιγραφή της εν λόγω περιοχής και του προγράμματος. Έπειτα περιγράφονται οι φυσικές αρχές σχετικά με τη ροή του νερού στο έδαφος. Συγκεκριμένα, μελετώνται οι ιδιότητες του εδάφους ως πορώδους μέσου, καθώς και της ροής της αποτελούμενης από δύο φάσεις, νερό και αέρα. Επίσης, συζητάται η ιδιαιτερότητα του εδάφους στη μελετώμενη περιοχή, δηλαδή οι μακροπόροι και η διαφορετική συμπεριφορά τους, οπότε προκύπτουν οι μαθηματικές εξισώσεις που τελικά χρησιμοποιούνται στο λογισμικό για να περιγράψουν τη ροή του νερού στο έδαφος. Εκτός αυτών, παρουσιάζονται τα διάφορα είδη μοντέλων που υπάρχουν για τη ροή νερού σε πορώδες μέσο και εξηγούνται η δομή και η λειτουργία του MUFTE-UG.

Σχετικά με τις εφαρμογές με το λογισμικό πακέτο, πρώτα περιγράφονται οι παράμετροι και οι παραδοχές που υιοθετούνται στην εργασία. Παρουσιάζονται το σκεπτικό και η μορφή των αρχικών αλλά και των οριακών συνθηκών στα σύνορα του πεδίου ροής, δηλαδή των οριακών συνθηκών Dirichlet και Neumann. Επίσης, παρουσιάζονται και σχολιάζονται οι προσομοιώσεις και αντιπροσωπευτικά αποτελέσματα. Ειδικά μελετώνται οι περιπτώσεις των οριακών συνθηκών Dirichlet και Neumann για το νερό στο πάνω όριο του πεδίου ροής. Τέλος, παρουσιάζεται λεπτομερώς μια επέκταση αυτών των δύο, η οριακή συνθήκη Rainfall.

Τα συμπεράσματα στηρίζονται σε προσομοιώσεις της διαδικασίας διήθησης για τις διάφορες συνθήκες, λαμβάνοντας υπόψη την ποσότητα και ταχύτητα διήθησης, καθώς και την αβεβαιότητα των υιοθετημένων παραμέτρων.

Summary

The present thesis deals with the investigation of boundary conditions in the simulation of water infiltration into ground with the simulation tool MUFTE-UG. This study is aiming to the application and further development of the software MUFTE-UG, in the frame of the Grosshang project in western Austria, concerning moving landslides.

A general description of the study area and the project is given first in the thesis. After that, the related physical principles are described, regarding subsurface flow. Specifically, certain properties of the ground as a porous medium are studied as well as flow consisting of two phases, water and air. Also the special feature of the ground at the studied area, the differently behaving macropores, is discussed, leading to the final form of the mathematical relations used in the program to describe subsurface flow. Apart from these, the existing model types for simulating water flow in a porous medium are presented and the structure and function of MUFTE-UG are explained.

As for the applications of the simulation tool, the parameters and assumptions concerning the study in the present thesis are firstly described. The concept and setup of the initial as well as the boundary conditions(BC) at the boundaries of the domain are then presented, namely the Dirichlet and the Neumann BC. The simulations and some representative results are given and discussed. Certain cases of Dirichlet BC and Neumann BC for the water at the top boundary are studied. An extension of the two, the Rainfall BC, is also presented and explained in detail.

Conclusions are based on simulations of the development of the infiltration process for the various conditions, in terms of quantity and velocity, as well as the uncertainty of the assumed parameters.

Author's Statement

I hereby certify that I have prepared this study independently, and that only those sources, aids and advisors that are duly noted herein have been used or consulted.

Signature

Date

Contents

1	Introduction	8
2	Grosshang Project	10
3	Physical Background	13
3.1	Water flow in porous media	13
3.2	Porous Media	13
3.2.1	REV Concept	14
3.2.2	Porosity	14
3.2.3	Saturation	15
3.2.4	Permeability	15
3.3	Two Phases	16
3.3.1	Saturation in a multiphase flow	16
3.3.2	Relative Permeability	17
3.3.3	Capillary Pressure	18
3.4	Macropores	19
3.4.1	Origin of Macropores	20
3.4.2	Macropore Flow and Modelling	22
3.5	Flow Equations	23
3.5.1	Continuity Equation and Darcy Law	23
3.5.2	Two Phase Flow Equations	24
4	Modelling Two-Phase Flow in Macroporous Media	26
4.1	Model Concepts	26
4.1.1	Equivalent Models	26
4.1.2	Discrete Models	27
4.2	MUFTE-UG	28
4.2.1	Equations and Parameters	29
4.2.1.1	Continuity Equation Formulation	29

4.2.1.2	Coupling two continua	29
4.2.1.3	Parameters of the double-continuum model	30
4.2.2	Boundary and Initial Conditions	33
4.2.3	Discretisation Methods	33
4.2.3.1	Time Discretisation	34
4.2.3.2	Spatial Discretisation	34
4.2.4	Approximation Methods	35
5	Setting the Study	36
5.1	Flow Principles	36
5.1.1	Flow Dimensions	36
5.1.2	Fluid Properties	37
5.2	Domain of Flow	37
5.2.1	Geometry and Ground Properties	37
5.2.2	Boundary and Initial Conditions	40
5.2.2.1	Boundary Conditions	40
5.2.2.2	Initial Condition	41
5.2.3	Discretisation Mesh and Results Visualisation	42
6	Forming an Initial Condition	43
6.1	Steady State Simulation	43
6.1.1	Setup	43
6.1.2	Results	44
7	Infiltration with Dirichlet and Neumann Boundary Conditions	47
7.1	Dirichlet BC Simulation	47
7.1.1	Setup	47
7.1.2	Results	48
7.2	Neumann BC Simulation	50
7.2.1	Setup	50
7.2.2	Results	51
7.3	Comparison	54
8	Infiltration with Rainfall Boundary Condition	56
8.1	Implementing a Rainfall Boundary Condition	56
8.1.1	Modelling the Rainfall BC	57
8.1.1.1	Implemented Quantities	57

8.1.1.2	Structure of the Boundary Condition	59
8.1.1.3	Assumptions	60
8.1.2	Relation to existing Boundary Conditions	61
8.2	Input from a Rainfall Event	62
8.2.1	Setup	62
8.2.2	Results	63
8.3	Comparing Rainfall and Neumann Boundary Conditions	67
8.3.1	Wet Humus Layer Model	67
8.3.1.1	Setup	67
8.3.1.2	Results	69
8.3.2	Rainfall Event Model	71
8.3.2.1	Setup	72
8.3.2.2	Results	72
8.3.3	Comparison	76
8.3.3.1	Rainfall vs Neumann above a Humus Layer	76
8.3.3.2	Rainfall vs Neumann	76
9	Conclusions	77
	Bibliography	79

List of Figures

2.1	Grosshang project	11
3.1	Upscaling to a Representative Elementary Volume (REV), modified after <i>Hinkelmann</i> [2005]	14
3.2	Relative permeability-water saturation relation for water and air, after <i>van Genuchten</i>	18
3.3	Capillary pressure-water saturation relation for three different soils, after <i>van Genuchten</i>	20
3.4	Macropores at Heumöser Hang (pictures taken by F.Lindenmaier, K.Germer, J.Wienhöfer)	21
3.5	Flow types in macropores, modified after <i>Hartge & Horn</i> [1999]	22
4.1	Model types, after <i>Neunhäuserer</i> [2003]	27
4.2	Numerical Simulator MUFTE-UG [<i>Hinkelmann</i> , 2005]	28
4.3	Double-continuum model [<i>Stadler et al.</i> , 2008]	30
4.4	Interface coupling matrix and macropores	31
4.5	Discretisation with element and box meshes (Box Method)	35
5.1	Domain of Study	38
5.2	Double- Continuum domain	38
5.3	Boundary conditions for the domain	41
5.4	Initial condition	42
6.1	Steady State simulation	45
7.1	Boundary conditions for the Dirichlet simulations	48
7.2	Dirichlet Simulation: (a) 30% saturation at matrix top boundary	49
7.3	Dirichlet Simulation: (b) 70% saturation at matrix top boundary	50
7.4	Boundary conditions for the Neumann simulations	51
7.5	Neumann simulation: $0.36 \frac{\text{mm}}{\text{h}}$ at matrix top boundary	53

7.6	Neumann simulation: $36\frac{\text{mm}}{\text{h}}$ at matrix top boundary	54
8.1	Rainfall boundary condition on top of the domain	57
8.2	Implemented surface length and pressure gradient	59
8.3	Flowchart for the Rainfall BC concept	60
8.4	Development of the applied rainfall event	63
8.5	Rainfall Event : 0-23 hours	64
8.6	Rainfall Event : 24-119 hours	65
8.7	Rainfall Event : 120-168 hours	66
8.8	Boundary conditions for the Humus Layer simulations	68
8.9	Humus Layer simulation: $0.36\frac{\text{mm}}{\text{h}}$ at the matrix top boundary	70
8.10	Humus Layer simulation: $36\frac{\text{mm}}{\text{h}}$ at the matrix top boundary	71
8.11	Boundary conditions for the Rainfall simulations	72
8.12	Rainfall simulation: $0.36\frac{\text{mm}}{\text{h}}$ at the matrix top boundary	74
8.13	Rainfall simulation: $36\frac{\text{mm}}{\text{h}}$ at the matrix top boundary	75

List of Tables

5.1	Ground Parameters	39
5.2	Van Genuchten Parameters	39
5.3	Permeability Values for Beta Parameters	40
8.1	Rainfall event inflow values	63

1 Introduction

Stability of mountain slopes is an issue concerning society in many ways, from safety of residential areas laying nearby, to the building and development prospects of mountainous regions. It is therefore important that it is controlled and potentially preserved by the respective engineers and scientists teams and institutes. For this reason, the German Research Society (Deutsche Forschungs Gemeinschaft- DFG) runs the Grosshang research project at the moving slope Heumös in Ebnet, Vorarlberg in western Austria. This project aims at the depicting and understanding of the dominant parameters of the slope's movement and their relations.

Specifically, slope stability depends on various factors, mainly on the consistency and geomorphology of the ground, seismic activity and water flow both on surface and underground. As far as water flow is concerned, there are complex interactions between surface runoff and groundwater flow, connected through infiltration processes and affected also by precipitation, vegetation, natural sources etc. In this field of the project, there are measurements being held in site, experiments being carried out in laboratories and simulation tools being developed.

Such a tool is MUFTE-UG (MULTIphase Flow, Transport and Energy- Unstructured Grids), a piece of software describing subsurface flow in a strongly heterogeneous porous medium, consisting of a relatively homogeneous soil matrix and remarkably larger pores, macropores. These variations of pore size often make water flow unpredictable, since water may be transferred into macropores and thus be infiltrated more quickly or bypass less permeable layers. As a result, time or even space scale of water flow may differ significantly, ranging from minutes to months, and from a local flow space to whole hills, causing respectively deformation of the slope sooner or later.

The target of this certain thesis is to investigate the complex coupling of the two continua, and in specific, various boundary conditions of the considered matrix, that describe different infiltration cases. The expression of the conditions that determine input values at the boundaries of the examined matrix is of considerable importance to solving the respective mathematical equations with physical consequence and time efficiency. Especially when the distribution of the water into the distinct media is taken

into consideration, the right conditions must be formed for both media. There are several models being tested, including reaching saturation equilibrium in the matrix, taking into consideration unstable layers on the top of the matrix and rainfall events. As for the latter, an extension was implemented to the existing program (MUFTE-UG), allowing precipitation to be considered as a special physical process, affecting the way of infiltration into the media.

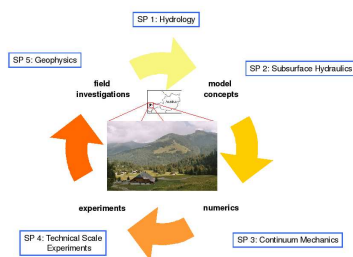
2 Grosshang Project

Vorarlberg is the westernmost district of Austria, well-known for its dairy industry and tourism, apart from its other industry activities, counting almost 370.000 permanent residents. A special feature of the region is its mountainous morphology, appropriate also for ski-resorts. Another characteristic is the high precipitation rates, reaching an average of 1900mm per year.

In this landscape, slow landslides have been noticed in the last years. Because of the importance of ensuring safety for both permanent residents as well as visitors, the German Research Society (Deutsche Forschungs Gemeinschaft- DFG) has been running a project since 2006, forming another research group, dealing with the Coupling of flow and deformation processes for modelling of large mass movements. In the so called Grosshang Project, institutes from the Universität Karlsruhe (TH), Universität Potsdam, TU Berlin, Universität Stuttgart, Universität Muenchen and Helmholtz Zentrum für Umweltschutz are involved. The activity of various research fields is required in the project, such as geosciences, geotechnics, hydraulics and subsurface hydraulics, in a wide range of time and spatial scales.



(a) Heumöser Hang, Vorarlberg, West Austria



(b) Multi-field cooperation

Figure 2.1: Grosshang project

As no appropriate simulation methods for the needed research exists, the aim of the

Grosshang research group is to suggest new solutions, using coupling, averaging and up-scaling methods, combined with deterministic and stochastic principles. Measures in-site and experiments in the laboratory in order to understand main processes involved and to obtain necessary values, are the first steps, followed by the development of simulation tools. The developed tools have to be controlled experimentally in the laboratory before applied on real field.

In the frame of the Grosshang Project, MUFTE-UG is used, as a simulation tool for subsurface flow. It was initially developed in Universität Stuttgart, as a multiphase flow simulator, and later extended in TU Berlin into a double-continuum model. Physical principles and values implemented are based on experiments held by Germer [*Germer et al.*, 2008], concerning infiltration in a single macropore. A more detailed description of the model is given in section4.2.

3 Physical Background

Water flow under land surface can be the reason for changes in the structure of ground particles, therefore tensions and maybe deformations.

Subsurface flow depends on many factors. In contrast to surface flow, it is not only the fluid itself that plays a significant role, but also the ground medium. This means that characteristics of the fluid and also of the ground determine the properties of the flow. In the following, the most important related parameters are being described and explained.

3.1 Water flow in porous media

Water from the surface, for instance in rivers or precipitation water, is able to infiltrate into the ground, because of ground's non-continuous nature. It can be held in the pores which are formed among the more consistent parts of ground formations, from grains to rock blocks. There, it can either fill these pores in hydrostatic state, which results in groundwater aquifers, or flow through connected pore channels, meaning possibly flow into and out of aquifers, representing flow in the unsaturated zone.

Regarding flow, as water moves from one point to another, there is loss of energy to be noticed, due to the fact that the medium particles can be simplified considered as obstacles to the water particles. Water must have this energy in advance, in order to be able to spend it. For this reason, a gradient of the hydraulic potential (if omitting more rare reasons of flow, such as chemical or electrical potential) of the water between two points is demanded so that water can flow from the one to the other. This gradient is described in more detail in section 3.5.1.

3.2 Porous Media

A porous medium is not a continuous medium as a usual material is considered to be in physics, but we could approach it as multiphase matter, consisting of solid phase and at least one non-solid phase, namely gas or liquid phase. The solid phase is then referred

to as solid matrix, whereas the rest of the space within the porous medium is called void space or pores, with usually at least some of them being interconnected. Examples of such media in the ground are soil materials, ranging from fine clay to grobe sand [Bear, 1988].

3.2.1 REV Concept

It is at least very difficult, and maybe unnecessary, to describe properties and processes of groundwater flow at a real microscale between grains and pores. For this reason, the most common concept of studying subsurface flow is considering a larger scale and averaging these processes. This upscaling refers to volumes called Representative Elementary Volumes or REVs. They are chosen so that the respective quantities are averaged in the most representative way, namely in general large enough, in order to avoid extreme fluctuations of the property, but also so small that significant spatial variations are taken into consideration [Hinkelmann, 2005].

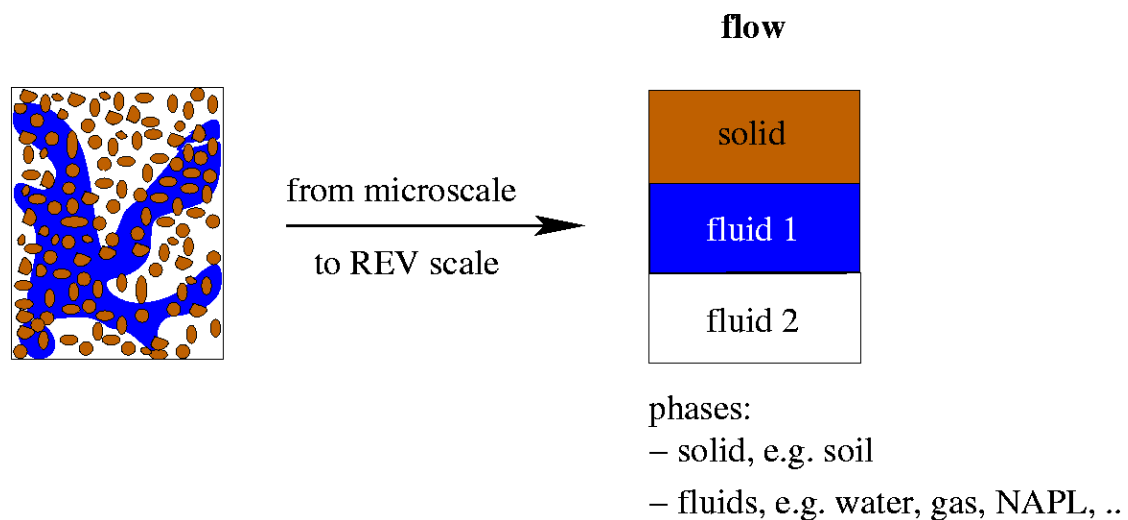


Figure 3.1: Upscaling to a Representative Elementary Volume (REV), modified after *Hinkelmann* [2005]

3.2.2 Porosity

A property of the REV describing an average consistency of the porous medium is porosity φ . It is defined as the ratio of the pore space within the REV and the total

volume of the REV:

$$\varphi = \frac{\text{pore space within REV}}{\text{total volume of REV}}. \quad (3.1)$$

It is a dimensionless quantity, expressed in percentages. Assuming that the solid matrix is non-deformable and neglecting temporal variations, the porosity remains constant and unaffected by temperature and pressure changes.

3.2.3 Saturation

The quantity that describes the part of the pores filled with fluid is Saturation S_a . It is defined as the ratio of the volume of the fluid in the pores within the REV and the total volume of the REV. It reads to

$$S_a = \frac{\text{volume of the fluid in the pores within the REV}}{\text{total volume of the pores within the REV}}. \quad (3.2)$$

More about saturation will be discussed in section 3.3.1.

3.2.4 Permeability

Flow in the REV is not determined by the porosity itself, namely the quantity of pore spaces, but also by the structure of the pores as well as fluid properties.

A property that refers to how easily a fluid can flow in a porous medium is hydraulic conductivity $\mathbf{K}_f [m \cdot s^{-1}]$. When one fluid is assumed as pore content, hydraulic conductivity is then defined as

$$\mathbf{K}_f = K \frac{\varrho \bar{g}}{\mu}, \quad (3.3)$$

where $\mathbf{K} [m^2]$ is the tensor of permeability or intrinsic or absolute permeability, $\varrho [kg \cdot m^{-3}]$ is the fluid density, $\bar{g} [m \cdot s^{-2}]$ the gravity constant and $\mu [Pa \cdot s = kg \cdot m^{-1} \cdot s^{-1}]$ the fluid viscosity.

Specifically, permeability K is a property of the solid matrix and takes into account the structure of the grains and consequently the distribution of the pores. This explains the low permeability of a clay of high porosity and the higher permeability of a sand of lower porosity.

As a consequence, assuming an incompressible fluid, hydraulic conductivity \mathbf{K}_f remains constant for the REV. If we also consider an isotropic continuum, K_f has the same value in the whole REV, so it can be simplified to a non-vectorial quantity.

In the case of multiphase flow, relative permeability k_{ra} is defined, which is being described in detail in section 3.3.

3.3 Two Phases

The pores are not always filled with only one fluid, but a two- or multiphase flow may occur, with two or more fluids, liquids or gases, for example with water and some pollutant. In the case of a groundwater aquifer, beneath aquifer level the pores are considered to be full of water, meaning a water saturation of 100%. Above this level, in the so called vadose zone, water saturation is lower, since the air included in the pores is also considered [Kavvas, 2007].

Specifically, each fluid, liquid or gas, in a multiphase system in the pore space of a REV is called a *phase*, if the single fluids are immiscible on the microscale and if they are separated by a clearly defined interface across which discontinuities in fluid properties exist [Helmig, 1997]. Depending on the contact angle between fluids' interface and solid surface, wetting and non-wetting phases can be distinguished. For contact angles between 0° and 90° , we refer to the fluid as the wetting phase, while for angles between 90° and 180° , as the non-wetting phase.

In the present thesis, the behaviour of water in the upper layers is studied, where exchange takes place into and out of the ground, namely in the unsaturated zone. Therefore the flow is referred to as a two-phase system of water and air, where water is always the wetting phase, being indicated with w , and air is the non-wetting phase, indicated with n .

We must then have separate expressions of properties and processes of flow for each phase. So saturation is for example calculated for each phase, and the equations of mass conservation and the Darcy law are also formed once for each phase.

3.3.1 Saturation in a multiphase flow

For more than one phases, we refer to the part of the pores being occupied by each phase separately. So saturation is then expressed as

$$S_a = \frac{\text{volume of the fluid in the pores within the REV}}{\text{total volume of the pores within the REV}} = \frac{\varphi_a}{\varphi}, \quad (3.4)$$

where the index a indicates a phase.

It is assumed that the total of the pore space is filled with fluids, consequently

$$\sum_a S_a = S_w + S_n = 1. \quad (3.5)$$

The saturation of some phase can change when the fluid is displaced by another fluid. The residual saturation of each phase S_{ra} refers to the part of the fluid that remains in the pores and cannot be extracted, but via phase transition. More precisely, such a displacement can occur because of either drainage or imbibition. Drainage is called the displacement process of a wetting phase through a non-wetting phase, in the present of water through air, while at imbibition a non-wetting phase is displaced by a wetting one [Bear, 1988]. During drainage, small amounts of the wetting phase can be held back in the fine pore channels, while during imbibition, small bubbles of the non-wetting phase may be entrapped by the incoming wetting phase and so be held back in the pores.

Taking into account the residual saturation of either the wetting or the non-wetting phase, there is also the effective saturation S_e of the wetting phase being defined. There are more than one definitions, used according to different constitutive relationships of relative permeability and capillary pressure (see sections 3.3.2 and 3.3.3 respectively). One of them includes the residual saturation of the wetting phase :

$$S_e = \frac{S_w - S_{rw}}{1 - S_{rw}}, \quad S_{rw} \leq S_w \leq 1, \quad (3.6)$$

while another includes both the residual saturation of the wetting and non-wetting phase:

$$S_e = \frac{S_w - S_{rw}}{1 - S_{rw} - S_{rn}}, \quad S_{rw} \leq S_w \leq 1 - S_{rn}. \quad (3.7)$$

3.3.2 Relative Permeability

In the case of a multi-phase system, and therefore of saturation lower than 1, the fluid does not flow so easily through the pores as when it fills them completely. This can be explained as the difficulty of the phase to displace another phase, at low saturation degrees. In this concept, the water phase in the upper layers of the ground above aquifer level moves with greater difficulty than in the aquifer, depending on its saturation.

This is expressed by the relative permeability k_{ra} , which is used as a dimensionless factor to the absolute permeability K of the ground. Hydraulic conductivity is then extended to the form

$$\mathbf{K}_f = k_{ra} K \frac{\rho \bar{g}}{\mu}, \quad (3.8)$$

which now refers to a certain phase a . While the absolute permeability K is a property of the solid matrix only, the relative permeability is determined by properties of the solid matrix as well as the phase saturation.

There have various relations been formed to describe this term, in relation to the phase saturation. The two most common of them have been developed by *Brooks and Corey*, and *van Genuchten*. In the present thesis the latter one is used:

$$k_{rw} = \sqrt{S_e} \cdot \left[1 - \left(1 - S_e^{\frac{1}{m}} \right)^m \right]^2 \quad (3.9)$$

$$k_{rn} = (1 - S_e)^{\frac{1}{3}} \cdot \left(1 - S_e^{\frac{1}{m}} \right)^{2m}, \quad (3.10)$$

where S_e is the effective permeability of the wetting phase and m a fitting parameter, calculated as in equation 3.13. This expression of relative permeability has been applied in a C algorithm [*Aitken & Jones, 2000*] for both phases and a general form of the curves is visualised in figure 3.2.

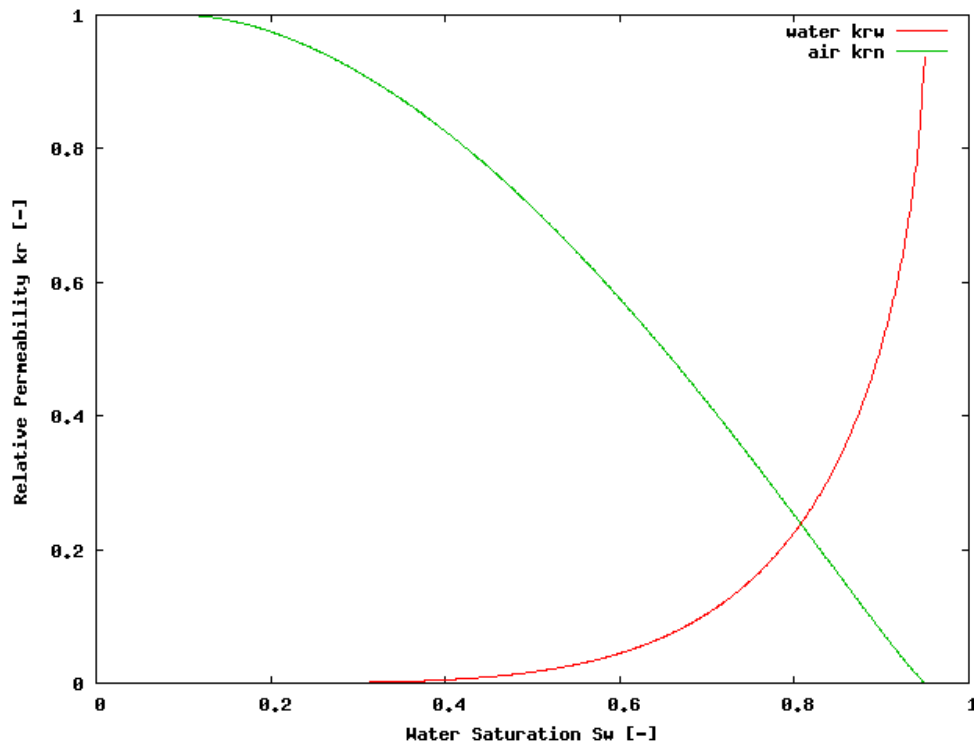


Figure 3.2: Relative permeability-water saturation relation for water and air, after *van Genuchten*

3.3.3 Capillary Pressure

At the interface of two immiscible fluids there can occur a difference of pressure between them. This difference results in interfacial tension, and possibly in a curving of the interface. Such a behaviour is to be observed at the aquifer level, or the interface between aquifer and the vadose zone, between water and air. Referring to a wetting and a non-wetting phase in general, this pressure difference is called capillary pressure p_c [Pa] and is defined as

$$p_c = p_n - p_w. \quad (3.11)$$

In a microscopic scale, capillary pressure can be formed based on the interfacial tension σ and the geometry of the fluid-solid matrix connection, reading then to:

$$p_c = \sigma \left(\frac{1}{r_x} + \frac{1}{r_y} \right) = \frac{4\sigma \cos \alpha}{d}, \quad (3.12)$$

as explained in *Bear* [1988].

In the macroscale on the other hand, capillary pressure can be regarded as a function of the wetting phase saturation. However, capillarity depends on more parameters, such as pore space geometry, fluid composition, etc. The expression of capillary pressure according to *van Genuchten* is adopted in MUFTE-UG:

$$p_c = \frac{1}{a} (S_e^{-\frac{1}{m}} - 1)^{\frac{1}{n}}$$

$$m = 1 - \frac{1}{n}, \quad (3.13)$$

where fitting parameters for the curve form a, n and m are derived from experiments.

As previously, plotted curves of the capillary pressure as a function of water saturation are presented, for various ground properties. In specific, the three curves in figure 3.3 correspond to the ground layers which form the domain of study in the thesis.

A point which should be paid attention to is the opposite development of the curves of relative permeability-water saturation and capillary pressure-water saturation as water saturation increases.

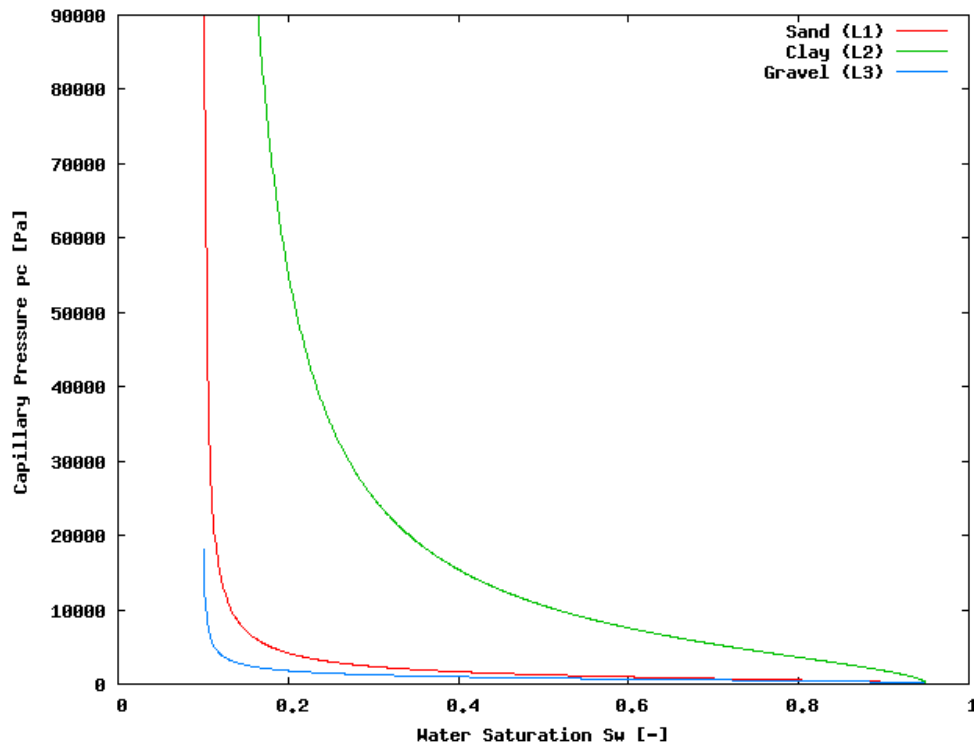


Figure 3.3: Capillary pressure-water saturation relation for three different soils, after *van Genuchten*

3.4 Macropores

Macropores, as a sort of fissure, can be found in plenty of cases in natural soils. Among many definitions of the macropores that can be found in the literature, the one given by *Jarvis* [2007] is adopted in the present thesis. Macropores are structural pores of large diameter, great continuity and little tortuosity, that allow the maintenance of lateral physical non-equilibrium conditions during vertical flow. From a functional point of view, pores larger than 0.3mm in equivalent cylindrical diameter can be considered as macropores.

Non-equilibrium conditions refer to a flow regime in which infiltrating water does not have sufficient time to equilibrate with slowly moving resident water in the bulk of the soil matrix. Therefore a spatially uniform precipitation flux becomes very non-uniform as flow streamlines converge towards conducting macropores, according to *Jarvis* [2007]. For this reason, not all large pores are macropores, since they have to fulfill also length, connectivity and tortuosity features in order to allow fast infiltration through them, and consequently non-equilibrium. Further characteristics of macropores are often coating

and lining of their surface, mainly due to clay and organic consistency.

3.4.1 Origin of Macropores

Macropores can be formed mainly as a result of biological and physical processes. According to their origin, their size and characteristics may vary.

Faunal origin is common to meet in macropores, resulting mostly from deep-burrowing earthworms [Shipitalo & Butt, 1999]. Flora can also be responsible for macropores. Decaying plant roots also create macropores, where a similar morphology to that of a living root system is often to be observed [Edwards et al., 1988]. Another possible reason for the forming of macropores is soil aggregation in soils containing swell/shrink minerals, when the cohesion of the soils is locally overcome due to wetting and drying or freezing and thawing [Jarvis, 2007].

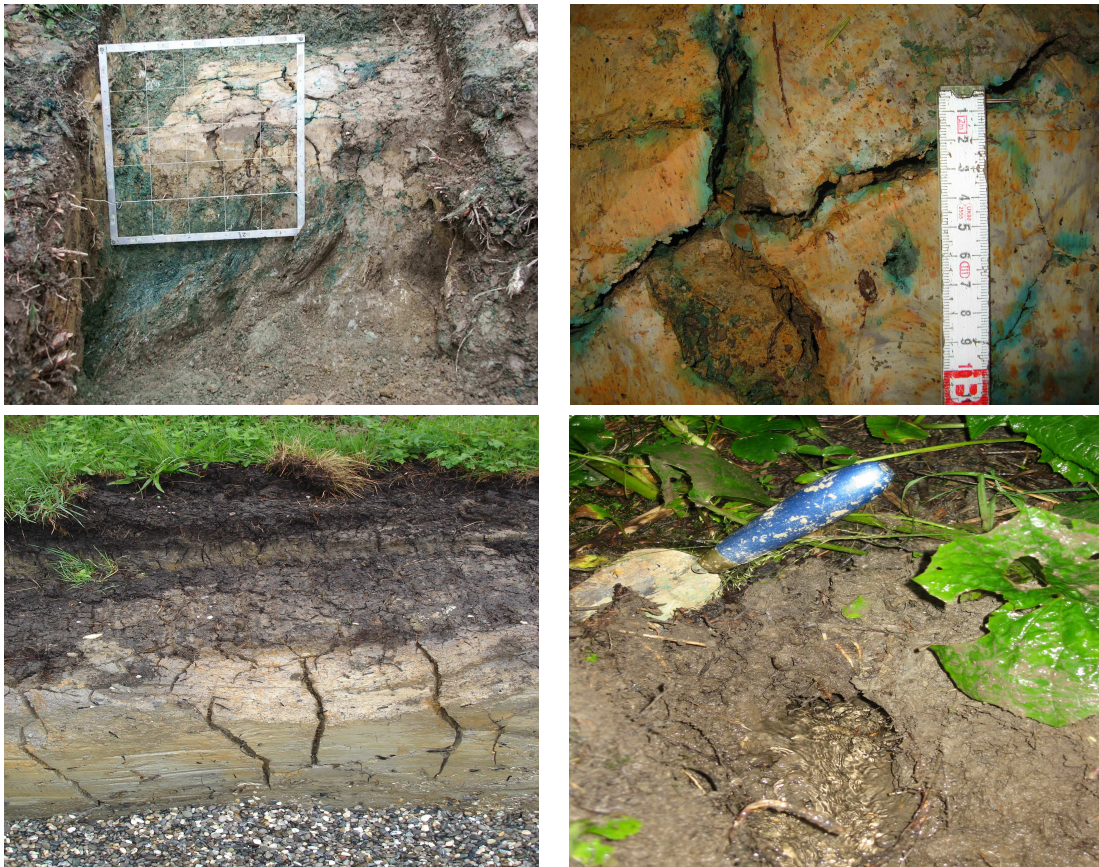


Figure 3.4: Macropores at Heumöser Hang (pictures taken by F.Lindenmaier, K.Germer, J.Wienhöfer)

As far as Heumöser Hang is concerned, there have been various fissures recognised, which fulfill the definition of macropores. Specifically, Lindenmaier reports about macropores, soil pipes and shrinkage cracks. Former root holes from marsh plants are the most dominant circular macropores found, with diameters of around 0.3 to 1.0cm . These roots can be opened to the surface in creek gullies and forest slopes. Soil pipes with a diameter of around 10cm were found in the southern and northern slopes, while it is not clear whether they return back to surface or not. Shrinkage cracks with a surface aperture of even 2.5cm are observable, caused in clays with high moisture contents during dry periods, because of their capability to shrink and change their volume significantly. In the course of this thesis, all of these fissures are considered as macropores since they allow water flow through them, functioning for instance as surface sources, according to *Lindenmaier* [2007].

3.4.2 Macropore Flow and Modelling

Macropores influence flow both in themselves and in interaction with the pores. Water flow through macropores is dominated by gravity, since capillarity is unlikely to become large, and flow velocities are considered slow enough, so that acceleration terms are neglected [*Jarvis*, 2007]. Based on this assumption, the Darcy law can be applied for macropore flow, as well as for pore flow (see 3.5.1).

The balance between the supply of water and exchange with the matrix determines the saturation degree and prevailing flow mechanism in macropores. 'Film' flow can take place along the macropores at low saturations. If the degree of saturation increases, capillary 'bridging' across the narrowest sections of varying-width fissures can occur, causing an intermittent 'pulse' flow, or equally 'plugflow' [*Jarvis*, 2007].

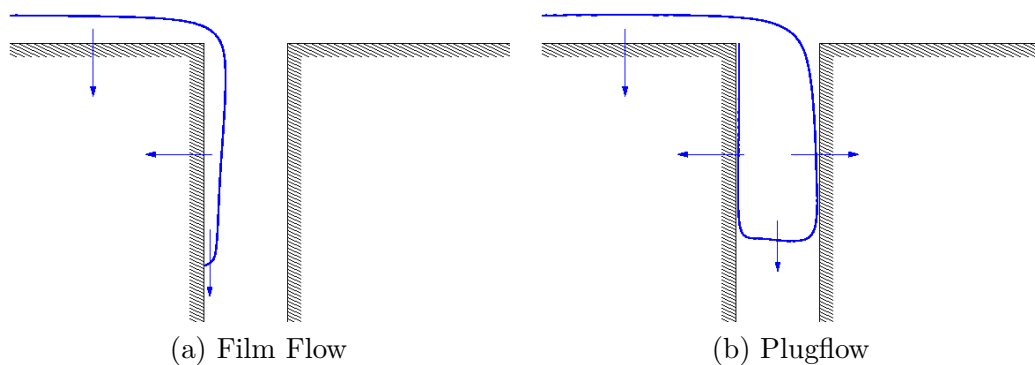


Figure 3.5: Flow types in macropores, modified after *Hartge & Horn* [1999]

Flow infiltration into macropores can on the one hand occur due to intense storms on initially dry soils [Edwards *et al.*, 1988], because of low initial mobility of the matrix (see 3.5.2). In spite of this, the flow concept in the present study is that water infiltrates first into the finer pores of the matrix, taking into account the low capillarity of the macropores. For this reason, the dominant infiltration into the macropores is the lateral one from the matrix. Specifically, water will start to flow into a macropore when the water pressure at some point on the interface with the surrounding soil matrix exceeds the 'water entry' pressure. As water starts to flow into large structural macropores, the sharp contrast in pore size and tortuosity with the surrounding matrix pores leads to an abrupt increase in water flow rate for only a small increase in soil water pressure [Jarvis, 2007]. In order for the flow to be sustained in the macropores though, vertical flow rates have to be large enough in relation to lateral losses into the matrix due to prevailing pressure potential gradient, as Germer *et al.* [2008] has realised through simulations of direct infiltration into a single macropore, where matrix imbibes water from the macropores.

Fast infiltration that can occur in the macropores has to be taken into account. Another important aspect of macropore flow is the bypassing of layers of small hydraulic conductivity, where the infiltration capacity of the matrix is exceeded and fast flow through macropores can cause pressure increase in deeper regions.

Taking into consideration the above mentioned, it is realised that the macropore flow has to be studied separately. As non-equilibrium processes take place, different pressures and possibly different motion equations are needed for matrix and macropores, resulting in a double-continuum approach. Apart from this, a two-phase flow is needed to be assumed, since fast infiltration of large amounts of water can lead to air entrapment, which in turn reduces the water infiltration significantly [Beven & Germann, 1982]. A detailed review on existing models for macropore flow is given by Simunek *et al.* [2002].

3.5 Flow Equations

Groundwater flow properties and processes are described by mathematical equations which mostly refer to a considered REV. Balance of flow quantities is examined in the certain REV, assuming their conservation, like the mass conservation and the momentum conservation. We are thereby led to equations such as the Continuity Equation and the Momentum Equation. Some mathematical expressions may also be derived experimentally, like the Darcy law.

3.5.1 Continuity Equation and Darcy Law

The continuity equation results from a macroscopic mass balance in the REV over the fluid mass, where parameters from microscale are averaged. Assuming that the average fluid mass flux is much larger than the deviations caused by microscale phenomena, such as diffusion and dispersion, these terms can be neglected. We then receive:

$$\frac{\partial(\varphi \varrho)}{\partial t} + \text{div}(\varphi \varrho \bar{v}_{aver}) - \varrho q = 0 \quad (3.14)$$

in the REV [Helmig, 1997]. The first term describes the change of the mass in the volume over time. In a stationary flow, there are no temporal changes, so the term can be omitted. The second term stands for the exchange of mass into and out of the REV through the boundary, with defined negative values in inflow cases. Here \bar{v}_{aver} is the average velocity, which takes into account the porosity of the medium, namely

$$\bar{v}_{aver} = \frac{\bar{v}}{\varphi}. \quad (3.15)$$

The last term includes the source ($\varrho q > 0$) or sink ($\varrho q < 0$) which may exist in the REV.

The Darcy law is an originally experimentally derived, macroscopic expression of the momentum equation. It requires slow laminar flow and reads to $\bar{v} = -\mathbf{K}_f \cdot \text{grad}h$, where the negative sign compensates for the negative gradient and $\text{grad}h$ is the gradient of the piezometric head h , the potential energy per unit weight of fluid. Specifically, piezometric head h is the sum of the pressure head $\frac{p}{\varrho g}$ and the elevation head z , namely

$$h = \frac{p}{\varrho g} + z. \quad (3.16)$$

So, equivalently,

$$v = -K \frac{1}{\mu} (\text{grad}p - \varrho g). \quad (3.17)$$

3.5.2 Two Phase Flow Equations

In a two phase system, each phase flow is described by a separate equation:

$$\frac{\partial(\varphi_a \varrho_a)}{\partial t} + \text{div}(\varphi_a \varrho_a \bar{v}_{aver}) - \varrho_a q_a = 0. \quad (3.18)$$

If we use the porosity of each phase φ_a instead of the total porosity φ , according to equation 3.4, namely

$$\varphi_a = S_a \varphi,$$

we obtain the continuity equation for each phase:

$$\varphi \frac{\partial (S_a \varrho_a)}{\partial t} - \operatorname{div} \left\{ \varrho_a \frac{k_{ra}}{\mu_a} K (\operatorname{grad} p_a - \varrho_a \bar{g}) \right\} - \varrho_a q_a = 0. \quad (3.19)$$

By further applying the quantity of phase mobility

$$\lambda = \frac{k_{ra}}{\mu_a}, \quad (3.20)$$

we finally use the following form of the continuity equation for each phase :

$$\varphi \frac{\partial (S_a \varrho_a)}{\partial t} - \operatorname{div} \{ \varrho_a \lambda_a K (\operatorname{grad} p_a - \varrho_a \bar{g}) \} - \varrho_a q_a = 0. \quad (3.21)$$

It is important to pay attention to the influence of the capillary pressure-saturation and the relative permeability-saturation relations on the pressure and the mobility terms respectively.

The continuity equations for wetting and non-wetting phases, meaning water and air phases respectively, is combined with the expression of capillary pressure and the phases' saturation relation, so that they are solved as for two unknowns. These unknowns are then called primary variables and depend on the formulation of the equations, which is chosen based on the special features of the problem studied. There are two formulations of the equation system regarding its variables:

1. wetting phase saturation S_w - non-wetting phase pressure p_n
2. wetting phase pressure p_w - non-wetting phase saturation S_n

As far as the first formulation is concerned, which is the one used in the present, if applying the equations

$$\operatorname{grad} p_w = \operatorname{grad}(p_n - p_c) \quad (3.22)$$

$$\frac{\partial S_n}{\partial t} = \frac{\partial}{\partial t} (1 - S_w) = -\frac{\partial S_w}{\partial t}, \quad (3.23)$$

the two continuity equations are obtained:

1. for the wetting phase

$$\varphi \frac{\partial (S_w \varrho_w)}{\partial t} - \operatorname{div} \{ \varrho_w \lambda_w K (\operatorname{grad} p_n - \operatorname{grad} p_c - \varrho_w \vec{g}) \} - \varrho_w q_w = 0 \quad (3.24)$$

2. for the non-wetting phase

$$-\varphi \frac{\partial (S_w \varrho_n)}{\partial t} - \operatorname{div} \{ \varrho_n \lambda_n K (\operatorname{grad} p_n - \varrho_n \vec{g}) \} - \varrho_n q_n = 0 \quad (3.25)$$

For more detailed presentation of the formulations, see *Helmig* [1997].

4 Modelling Two-Phase Flow in Macroporous Media

In order to model flow in subsurface systems, an appropriate conceptual model is at first needed. Afterwards, the mathematical equations formulated properly can be simulated. In this specific study, MUFTE-UG is the program used to simulate the considered equations.

4.1 Model Concepts

Two main model concepts exist for multiscale subsurface problems, the equivalent and the discrete ones, as well as hybrid models as combination of both.

4.1.1 Equivalent Models

Equivalent model concepts are based on the REV concept and assume that inhomogeneous domain can be considered as homogeneous bit by bit if shifting the observation scale. There are three main approaches of equivalent model concepts, the single-continuum, the double-continuum and the multi-continua. The most appropriate one of them is chosen depending on the spatial scale of the problem or maybe on the data available [Hinkelmann, 2005]. Namely, the more the length scales of discontinuities in the domain, such as fissures and fractures, vary and the less accurate the description of the discontinuities is, the more continua we need for modelling the flow. More specifically, single-continuum models are suitable for the case of similar scale fissures, so they are described as one equivalent porous medium. Double-continuum models are used respectively to describe two interacting continua consisting of a porous matrix with high storage capacity and low permeability and of macropores with high permeability and low storage capacity.

In a double-continuum model, the hydraulically very different components of matrix and macropores are treated separately and therefore described by two overlapping and interacting continua, the interaction between which is described by source or sink terms.

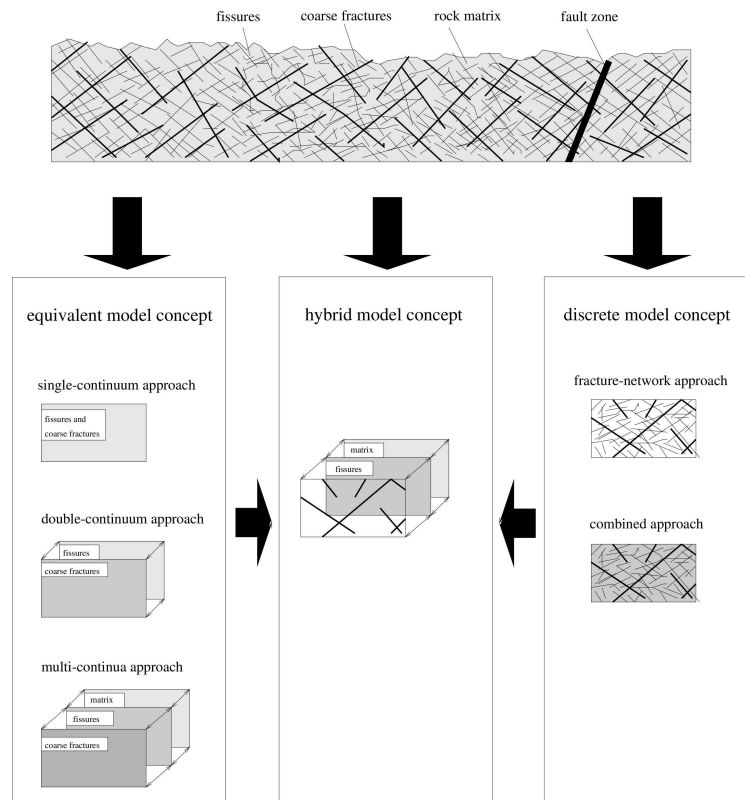


Figure 4.1: Model types, after *Neunhäuserer* [2003]

So at any point of the domain two values of each flow parameter are defined: one for the porous matrix and one for the macropore network. In the case of two continua, a dual-porosity and a dual-permeability model can be distinguished. In the first one the matrix functions as a storage continuum due to low hydraulic permeability. In the present model, assuming that the matrix has a pretty significant hydraulic conductivity and that flow in it can not be neglected, a dual-permeability model is applied. The system of flow equations then must be solved for each continuum separately.

4.1.2 Discrete Models

Discrete model concepts take into account the dominant fractures in the flow domain. Here the macropores must be described in detail and for this reason detailed information about their geometry and properties is required. Single-fracture, fracture-network and combined approaches can be distinguished. In single-fracture and fracture-network

models, the rock matrix is considered impermeable and thus non-interactive with the fractures. In a combined approach, both fractures and rock matrix are taken into account. The matrix can be an equivalent continuum of a fracture system on a smaller scale. The coupling of fracture and matrix is carried out by adding up fluxes in the Finite Volume Method, and by adding up parts of the local system matrices in the Finite Element Method [Hinkelmann, 2005].

4.2 MUFTE-UG

MUFTE-UG is a software package, which provides a double-continuum model for multiphase subsurface flow. Namely it simulates separately the porous matrix and the macropore network, and it takes into account the unsaturated zone near ground surface. It specifically solves numerically the continuity equation, in combination with the constitutive relations for capillarity and relative permeability, for each phase and for both continua. This is achieved by discretisation of the domain through the Box Method (Vertex-Centred Finite Volume Method), which is a combination of Finite-Element and Finite-Volume Methods, a fully implicit time discretisation and approximation of the solution by Newton-Raphson procedure.

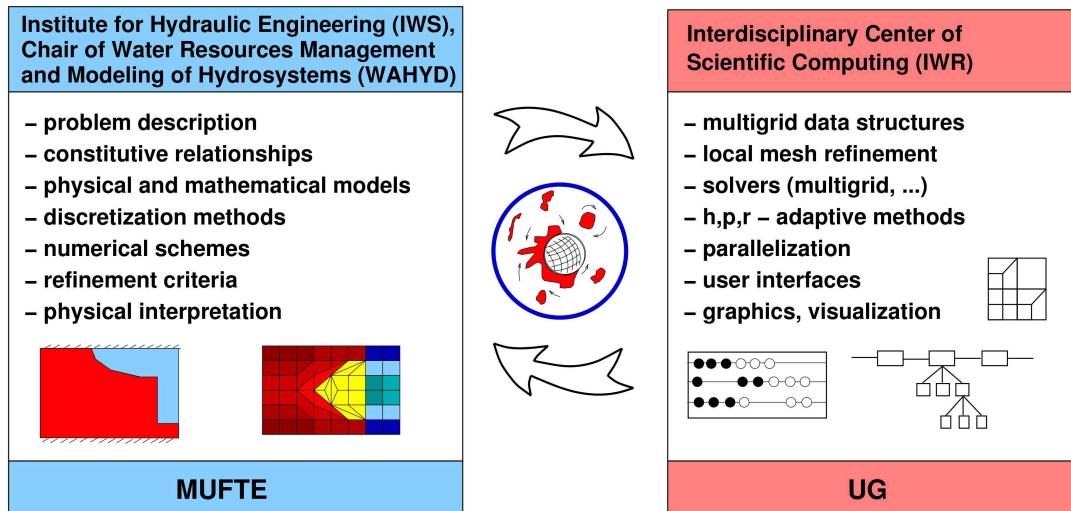


Figure 4.2: Numerical Simulator MUFTE-UG [Hinkelmann, 2005]

It is a combination of two toolboxes, MUFTE (MULTiphase Flow, Transport and Energy model) and UG (Unstructured Grid). The first one describes the physical part of

the flow problem as well as discretisation methods, while the second one is responsible for providing fast numerical solvers and handling the mesh [Stadler *et al.*, 2009].

4.2.1 Equations and Parameters

In MUFTE-UG two different formulations are applied, using as primary variables the saturation of one phase S_w or S_n and the pressure of the other one p_n or p_w respectively, and leading therefore to a pressure-saturation formulation.

4.2.1.1 Continuity Equation Formulation

In this study the formulation applied is as to water saturation S_w and air pressure p_n , since otherwise the constantly changing water pressure p_w would make the solution more complicated. Apart from that, an atmospheric pressure is desired, which can easily be defined by air-pressure (see section 3.5.2).

Attention should be paid to the strongly coupled nature of the equations and therefore to the fact that they must be solved simultaneously. It is also important to take into consideration the influence of the capillary pressure-saturation and the relative permeability-saturation relations, since the two quantities based on changes of the saturation of the phases develop in opposite ways to each other. This means that when for example water saturation rises, the capillary pressure declines while its relative permeability also grows bigger.

4.2.1.2 Coupling two continua

Since MUFTE-UG handles with two continua, the matrix and the macropores are set as two separate components of the studied REV. The considered dual-permeability means that both matrix and macropores contribute to the subsurface flow and consequently the continuity equation system must be applied twice, once for each continuum.

Apart from these, there are also coupling equations needed, namely describing the mass exchange between matrix and macropores continua. This leads to the implementation of one more continuity equation for each continuum, where the total mass flux must be equal in both balance equations. Specifically,

$$\varphi^m \frac{\partial (S_a^m \varrho_a^m)}{\partial t} + \text{div} (\varrho_a^m v_a^m) - \varrho_a^m q_a^m = \Gamma_a \quad (4.1)$$

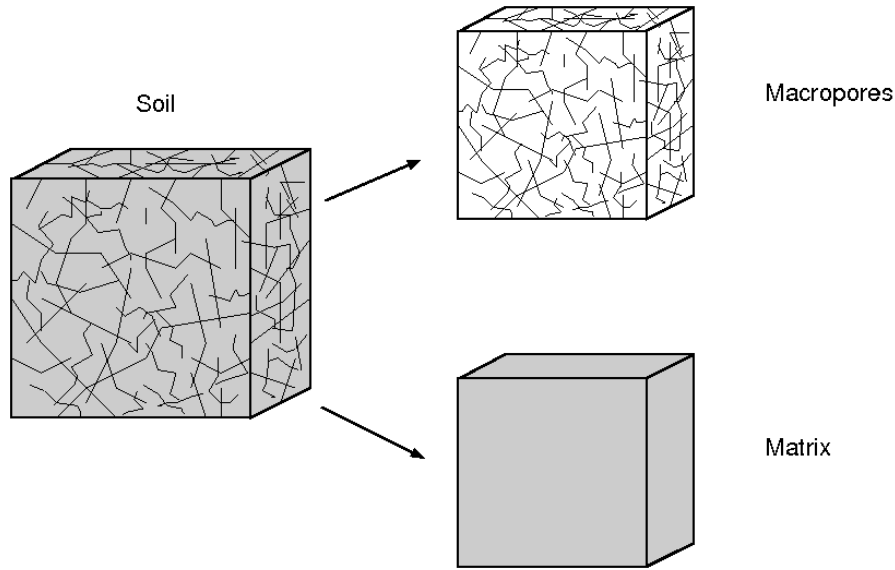


Figure 4.3: Double-continuum model [Stadler *et al.*, 2008]

$$\varphi^p \frac{\partial (S_a^p \varrho_a^p)}{\partial t} + \text{div} (\varrho_a^p v_a^p) - \varrho_a^p q_a^p = -\Gamma_a \quad (4.2)$$

where the superscripts m and p stand for the matrix and the macropores respectively, Γ_a is the flux of phase a exchanged between the two continua and the mass exchange is included in the second term. The mass exchange, as presented in the equations above, is not taken into account as a source-sink term, but is calculated as a flux term over the interface connecting the two continua.

The exchange interface is represented by the surface of the macropores A_{il} and is considered as an inner boundary condition in the simulation of MUFTE-UG. The macropore surface usually can not be known and described adequately in terms of geometry and distribution, and is therefore based on experimental results and geostatistical methods.

4.2.1.3 Parameters of the double-continuum model

Exchange Interface A_{il} The macropore surface A_{il} is considered as the interface between the two continua of the model. In order for the flow in both of them to be coupled, it must satisfy the continuity at the boundary, and namely

1. the total mass exchange must be equal to zero, or

$$\Gamma_a^m - \Gamma_a^p = 0 \quad (4.3)$$

2. the capillary pressure must be at any point of the interface the same on both sides, since it is a continuous variable, meaning

$$p_c^m = p_c^p. \quad (4.4)$$

The second condition is difficult to be fulfilled, as there has to exist a gradient of pressure at the exchange area between the two continua. To this end, a length l_{il} has to be introduced for the interface. In this way, the capillary pressure on the one side equals the value of the capillary pressure at the boundary of the porous matrix, while on the other side this one of the macropores, and in the interface a linear distribution between the two sides is assumed.

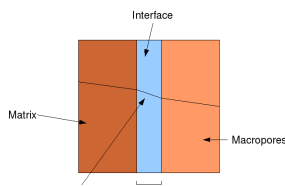


Figure 4.4: Interface coupling matrix and macropores

This length is no natural quantity, therefore it cannot be measured experimentally. For this reason studies have to be carried out applying arbitrary values, in order to match the scale of the domain.

Exchange Parameter β The mass exchange through the interface A_{il} is approached by a Darcy like flow relation, proposed by *Gerke & van Genuchten* [1993]. To this formulation, a gradient of pressure must be formed between matrix and macropores, dividing the difference of pressure in both continua by the implemented length of the interface l_{il} and permeability values must be given to the interface. Then we obtain

$$v_{a,il} = K_{il} \frac{kra}{\mu} \left(\frac{p_a^m - p_a^p}{l_{il}} \right). \quad (4.5)$$

The absolute permeability of the interface K_{il} can not obtain realistic values since experimental data is very rare. Though values can be received if the arithmetic average of the permeability of matrix and macropores is applied:

$$K_{il} = \frac{K^m + K^p}{2}. \quad (4.6)$$

Another concept for giving values to interface permeability is applying the harmonic average. The macropore surface is often biologically highly active soil area [*Jarvis*, 2007] and the macropores often origin from old plant roots, and therefore decreased permeability is to be expected. For this reason, as also because of potentially high heterogeneity between matrix and macropores, a harmonic average of the permeability of the two continua could be more suitable:

$$K_{il} = \frac{2K^m K^p}{K^m + K^p}. \quad (4.7)$$

It is though not always adequate to assume such values for the interface permeability, but experiments should be carried out to obtain those. Otherwise further concepts could be developed, taking into account the nature of macropores and their relation to the porous medium, like for example the fact that they pass through all ground layers in the heterogeneous domain.

As a consequence, there are two quantities in the velocity equation which cannot receive real values. In order to overwind this obstacle, a new fitting parameter is introduced, called Exchange Parameter β [m], which combines both permeability and length of interface, and expresses the convenience with which the mass flows through it:

$$\beta = \frac{K_{il}}{l_{il}}. \quad (4.8)$$

The exchange parameter β should be obtained from laboratory experiments, since the above suggested methods of giving K_{il} a value would produce further error.

Finally, if introducing also the mobility of the phase λ_a and the exchange parameter β , the velocity equation for the interface is formed:

$$v_{a,il} = -\beta\lambda_a (p_a^m - p_a^p). \quad (4.9)$$

Scaling Parameter For the coupling of the two continua, a scaling parameter is used, in order to take into account the total surface of macropores, through which the exchange takes place. Specifically, the *scaling* parameter is defined as:

$$scaling = \frac{\text{macropore surface}}{\text{volume of the domain}}.$$

The flux between the two continua is calculated as the flux between the sub-control volumes, multiplied by the *scaling* parameter, so as to obtain the exchange surface, and then multiplied by the interface velocity $v_{a,il}$ (see section 4.2.1.3).

4.2.2 Boundary and Initial Conditions

In order for the differential equations to be solved, certain values must be given at the boundaries, representing the interaction with the surrounding domain, as well as at initial time step, connecting the solution with the initial state.

The continuity equation used in MUFTE-UG is a partial differential equation. The solution function is prescribed along the boundary through a Dirichlet BC. If, otherwise, the derivative of the solution function in the direction of the exterior normal vector across the boundary is given, the boundary condition is a Neumann one [Hinkelmann, 2005]. A general example making clear the practical difference of the two conditions is that in a heat transfer problem, the temperature would be set at a constant degree at the Dirichlet BC, while the amount of heat transferred would be given at the Neumann BC. These are the two most commonly used boundary conditions in MUFTE-UG. As for the initial conditions, they are given in the form

$$e(x, y, z, t = 0) = e_0(x, y, z) \quad (4.10)$$

for a quantity e changing in time.

4.2.3 Discretisation Methods

The equation system of the model is solved based on discretisation of the domain and numerical approximation of the primary variables. The methods adopted are described next.

4.2.3.1 Time Discretisation

A one-step finite difference concept is applied for time discretisation. This means that the solution of the equations in every next time step $n + 1$ is based on values from the same time step $n + 1$. For instance, if

$$\frac{\partial e}{\partial t} = f(e) \quad (4.11)$$

an ordinary differential equation, then a time discretisation scheme with time step Δt^n leads to

$$\frac{e^{n+1} - e^n}{\Delta t^n} = f(e^{n+1}). \quad (4.12)$$

Because of this one-step relation, the method applied is a fully implicit method [*Hinkelmann, 2005*].

4.2.3.2 Spatial Discretisation

As far as spatial discretisation is concerned, the Box Method is applied in MUFTE-UG. It is namely a combination of Finite Elements and Finite Volumes Methods. The domain is discretised in two meshes, one consisting of finite elements and a second one consisting of finite volumes. Each element is defined by a rectangular with corner nodes i, j, k, l , which are used as the centres of the boxes of the volume mesh, as displayed in figure 4.5. In this way, the values of the variables are known at the nodes, but also the flux over the boxes boundaries is known.

Specifically, the variables are described exactly only at the nodes of the finite elements, while inbetween they are approximated through linear ansatz functions N_h (see *Paul & Class*). In a concrete example of the phase pressure

$$\tilde{p}_a = \sum_{h \text{ nodes}} \hat{p}_{ah} N_h, \quad (4.13)$$

\tilde{p}_a is the approximated value, \hat{p}_{ah} the discrete value at node h and N_h the ansatz function. Using the approximated values in the continuity equation results in an error ε . In order to take this into account, we demand that its product with a weighting function W_h integrated over the whole domain equals zero, namely

$$\int_G W_h \varepsilon dG = 0, \quad h = 1, 2, \dots, n \text{ nodes}. \quad (4.14)$$

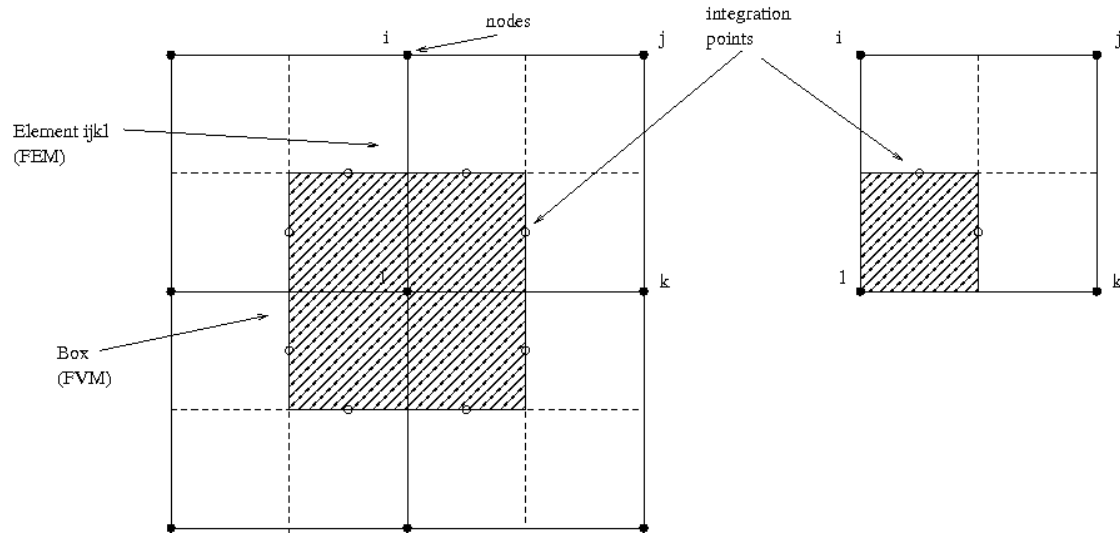


Figure 4.5: Discretisation with element and box meshes (Box Method)

It is due to this error that the procedure based on FEM is considered as locally non-conservative, and referring to the domain, globally conservative.

On the other hand, the gradient of the phase pressure p_a and the velocity v_a are calculated at the integration points at the boxes' boundaries of the finite volume mesh. Since flux values are also known, the FVM provides the process also with local conservativity (see *Helmig*). Thus the used Box Method is locally and globally conservative.

4.2.4 Approximation Methods

As already mentioned, the system of equations is highly non-linear, for which reason it is solved numerically. Newton-Raphson is used at each step to approximate through a circuit process the values of the partial differential equations. This means that the solution is not the exact one, and for this reason an error occurs. The reached solution at a time step is sufficient, when it results in an acceptable error. The proceeding followed is illustrated next for a random partial differential equation:

$$f(u) = 0$$

$$u^{n+1} = u^n - \left(\frac{\partial f}{\partial u}\right)_n^{-1} f(u^n), \quad (4.15)$$

where u a primary variable vector, $\frac{\partial f}{\partial u}$ a Jacobian matrix and n the current iteration step. An overview of numerical technics with Python is offered in *Kiusalaas* [2005].

5 Setting the Study

As mentioned before, the aim of this thesis is mainly to simulate various boundary conditions, so as to study their influence on physical processes of subsurface water and possibly adjust them further, extending thus the numeric simulator MUFTE-UG. For this reason, simple cases of flow and domain are examined regarding geometrical and physical characteristics, so that observations focus on concerned properties. Flow domain and properties are the same in all calculations presented later on, so that comparability of the results is ensured.

5.1 Flow Principles

It is previously explained that MUFTE-UG uses one continuity equation for each of both phases and for each of both continua in combination with the Darcy law and capillary pressure and relative permeability constitutive relations. In the present thesis, the formulation of water saturation-air pressure $S_w - p_n$ is applied.

5.1.1 Flow Dimensions

Flow is here always considered as single dimensional (1D), in a in two dimensions (2D) discretised soil column. The reason for this is that the infiltration through surface is the main object of interest, which is assumed in the vertical direction. In this way, the boundary controlling this exchange with surface water, which is the one on top of the domain, can be studied unaffected by the lateral boundaries and complex combinations of flow in more directions. It is also important that the discretisation grid is easier to control in 1D flow. Additionally, the main physical principles on which flow study is focused are capillarity and gravity, both macroscopically in vertical direction. Regarding mass exchange between both continua, it takes place through the interface A_{il} , as explained in section 4.2.1.3, which does not affect the one dimension of the flow in each continuum.

5.1.2 Fluid Properties

As far as fluids are concerned, air, referred to as non-wetting n phase, is assumed to be compressible. This takes into account the behaviour of the phases during the processes of replacement between them and is therefore a more realistic approach of the two-phase flow.

5.2 Domain of Flow

The REV used is a stratified double-dimensional domain. Both porous matrix and macropore network belong to REV's of the same dimensions.

From now on, the porous matrix will be referred to as continuum 1 (C1), while the macropores as continuum 2 (C2).

5.2.1 Geometry and Ground Properties

The domain width is chosen equal to 0.4m , the height to 3m , while in the z axis a constant length of 1m is assumed. It consists of three layers with varying hydraulic properties. The upper layer, layer 1, is loamy sand of intermediate permeability $K1$, the medium layer, layer 2, is clayey silt of low permeability $K2$, and the lower layer , layer 3, is gravel of high permeability $K3$. The medium layer was given the lowest permeability, so that it can potentially act as a linse with consequent bypassing through the macropores. So, for the permeability values:

$$K2 < K1 < K3.$$

The values of permeability as well as of porosity were derived as suggested values of these types of ground from tables of *Cirpka*, and presented in table 5.1. The domain is presented in figure 5.1, as a two dimensional column. In figure 5.1, the domain as assumed in the double-continuum model is given, where the matrix column, the macropores column and the interface can be distinguished.

Macropores were given a high permeability and a low porosity value, based on their large diameter and ability of fast infiltration. These values were derived by experimental data, carried out by *Germer et al.* [2008]. Macropore permeability is lower than the layers of the domain.

As far as the Van Genuchten parameters are concerned, they were fitted based on *Cirpka*, with values as shown in table 5.2.

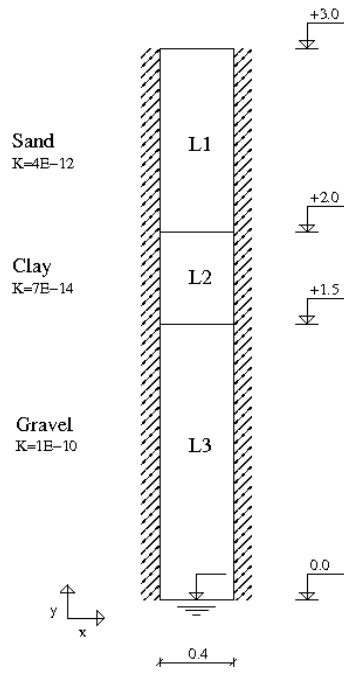


Figure 5.1: Domain of Study

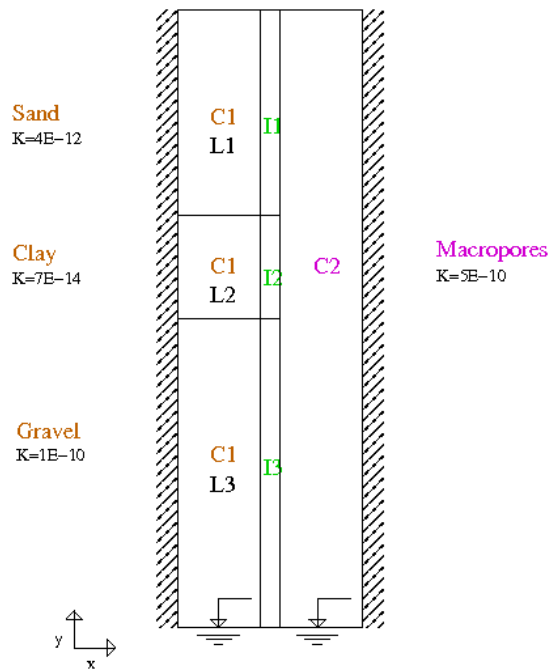


Figure 5.2: Double- Continuum domain

	sand	clay	gravel	macropores
porosity φ	0.4	0.5	0.3	0.05
absolute permeability K	4.05E-12	7.22E-14	1.0E-10	5.0E-10
residual water saturation S_{rw}	0.1	0.1	0.1	0.09
residual air saturation S_{rn}	0.05	0.05	0.05	0.05

Table 5.1: Ground Parameters

	sand	clay	gravel	macropores
a	12.6E-4	1.9E-4	16.0E-4	20.0E-4
n	2.28	1.9	3.0	4.0
m	0.56	0.47	0.67	0.75

Table 5.2: Van Genuchten Parameters

Regarding the interface A_{il} , three areas of interaction between continuum 1 and 2 can be distinguished, one for each layer. An exchange parameter β is set for each interface area, namely for each layer. Due to lack of experimental data, as explained in section 4.2.1.3, values have been assumed for the permeability of the interface K_{il} and calculations were carried out using initially three different combinations of exchange parameters:

1. the harmonic average of permeability of the matrix layer and the macropores, at each point
2. a lower permeability value than the absolute one for each layer
3. a common -though arbitrary- value lower than the one of the layers' lowest permeability

Table 5.3 contains the applied values of K_{il} as the exchange parameters. The applied values, as shown above, were chosen with regard to the form of macropores, consisting of coatings and linings on their surface (see section 3.4), and assuming their overall spreading in the domain. It is therefore sensible to assume hardened surface between pores and macropores and therefore a smaller permeability than in the continua. However, after realising no spectacular differences and for sake of time optimisation of the calculations, the harmonic averages were finally used in all calculations presented in the following.

K_{il}	sand	clay	gravel
1. harmonic average	8E-12	1.4E-13	1.7E-10
2. lower than absolute permeability	1.0E-13	1.0E-15	1.0E-11
3. common low	4.0E-15	1.0E-15	1.0E-14

Table 5.3: Permeability Values for Beta Parameters

5.2.2 Boundary and Initial Conditions

One boundary condition is used for each boundary, namely in total four boundary conditions have to be formed, two horizontal and two vertical ones. The initial conditions have to be set respectively for each one of the sub-domains, namely for the three layers in continuum 1 and for the macropores in continuum 2.

5.2.2.1 Boundary Conditions

The common boundary conditions applied in all simulations at the vertical and horizontal boundaries are depicted in figure 5.3.

At the vertical boundaries, a Neumann BC of zero inflow is applied in all cases. This ensures no lateral flow of wetting or non-wetting phase, and therefore a 1D flow. A Dirichlet BC here would represent impermeable boundaries and a hydrostatic pressure distribution for water, which would also add the difficulty of controlling the changes in this hydrostatic pressure during flow process because of changes in saturation.

At the horizontal bottom boundary, a Dirichlet BC is applied. For water, complete saturation is set, while for air, atmospheric pressure is assumed. This represents a free surface level of the aquifer, and ensures that all calculations simulate flow in the unsaturated zone.

At the horizontal top boundary, air is always described by a Dirichlet BC of atmospheric pressure, so that a free exchange surface is assumed. As for water, it obtains a Neumann zero flow over top surface in the macropore part of the REV, since water is assumed to infiltrate at first into the finer and thus with higher capillarity pores of the porous matrix. More about BC on the top boundary are discussed on certain calculation presentations later.

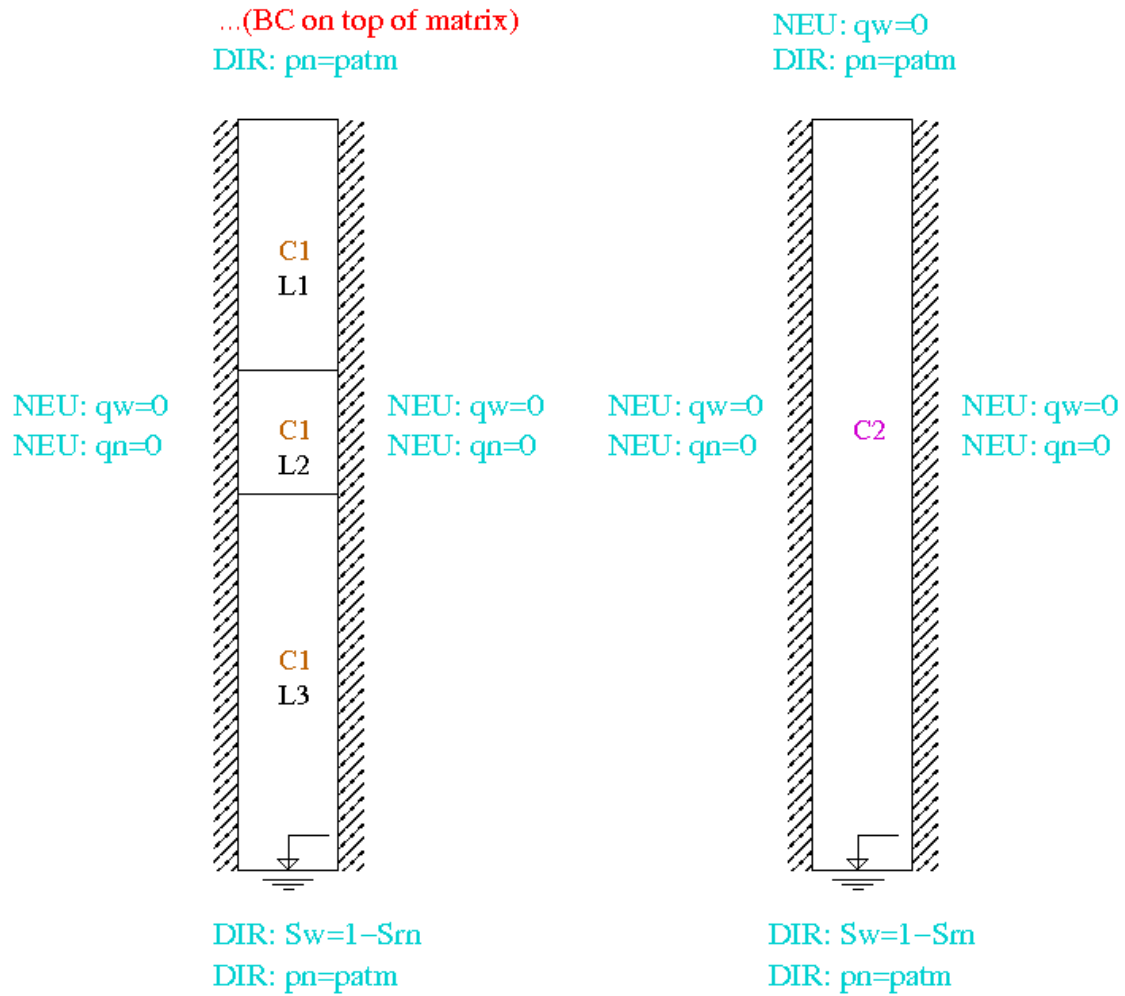


Figure 5.3: Boundary conditions for the domain

5.2.2.2 Initial Condition

Initially the ground is assumed to contain water saturation S_w , distributed in the layers according to their hydraulic and capillary properties. This image of water saturation distribution is achieved through a simulation presented in section 6.1. There, the less permeable a layer is, the higher water saturation rate is reached. Therefore, the medium layer has the highest saturation, followed by the upper one and last of the lower one, as shown in figure 5.4. The physical processes involved until this saturation distribution is reached are explained for a similar model by *Gisi et al.* [1997].

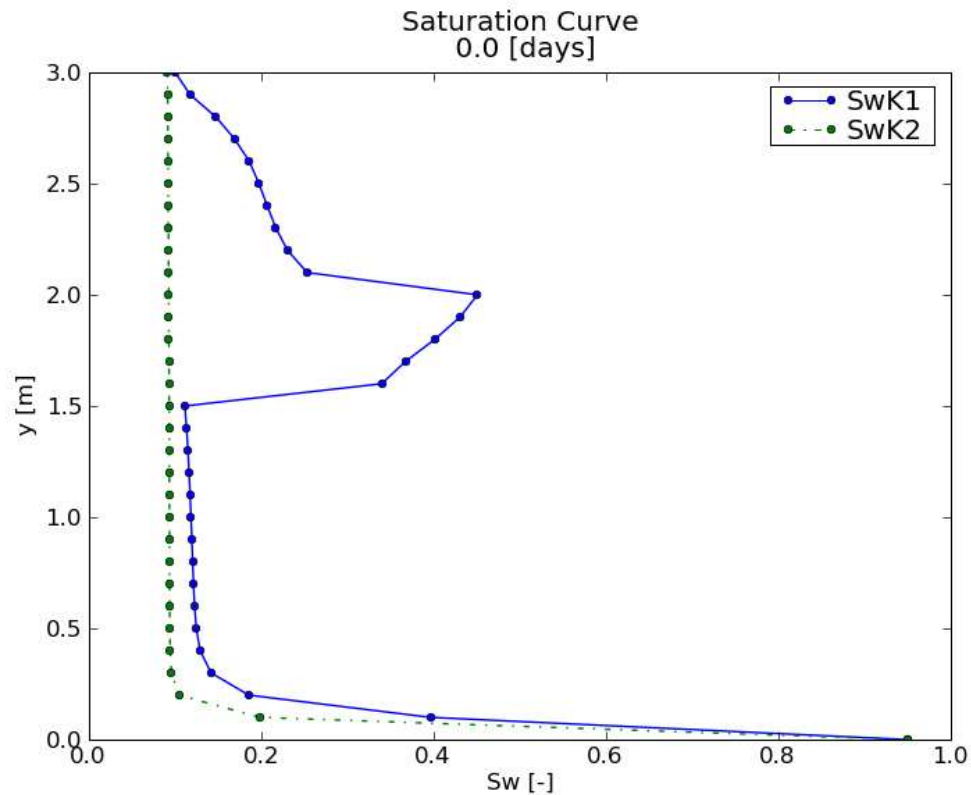


Figure 5.4: Initial condition

5.2.3 Discretisation Mesh and Results Visualisation

The simple form of the domain allows a simple and easy to supervise grid form. Specifically there have been four cells, each 0.1m wide, in the horizontal direction x and thirty cells, each 0.1m high, in the vertical direction y . The accuracy of the calculation would of course be higher by use of a more dense node network, but the time requirements of this would be beyond the aims of the present thesis.

Calculations results are visualised either as 2D columns by visualising tool Paraview or as cross sections by in python developed plotting software using matplotlib, where a development of the effective quantities during flow is displayed.

Apart from these, a useful method of controlling the mass flux in the vertical direction is the application of a Fluxline, a horizontal line implemented in MUFTE-UG, which can be activated and calculate the mass flowing over it at every time step.

6 Forming an Initial Condition

When an infiltration event occurs, the ground contains usually already some water in its pores depending on the hydraulic properties of the ground and its sub-domains. Such a state of water content was chosen as an initial condition for the calculations presented in this study. To its derivation simulations were carried out in both a single- and a double-continuum model. In this model various exchange parameters β were applied, so that the most appropriate of them were chosen for the next simulations.

6.1 Steady State Simulation

If assuming water in the pores of the domain and no interaction with the surface, the water is drained, while a part of it is held in the pores due to capillarity. This state is tried to be achieved in the next simulations.

6.1.1 Setup

The geometry of the domain and ground properties are the ones described in section 5.2.1. As for the exchange parameters β , various cases were studied, for some of which the permeability values K_{il} were used:

- two orders of magnitude larger than the respective permeability of the layers and two orders smaller than these
- the same values as the permeability of the layers
- the arithmetic averages of the permeability of the layers and macropores at every place
- the harmonic averages respectively
- lower values than the ones of the permeability of the layers

The boundary condition for water on top of the porous matrix was set as a Dirichlet BC of the residual saturation of water, so flow water is only the initially existing in the

pores. As an initial condition, a saturation of 0.3 was applied for both porous matrix and macropores.

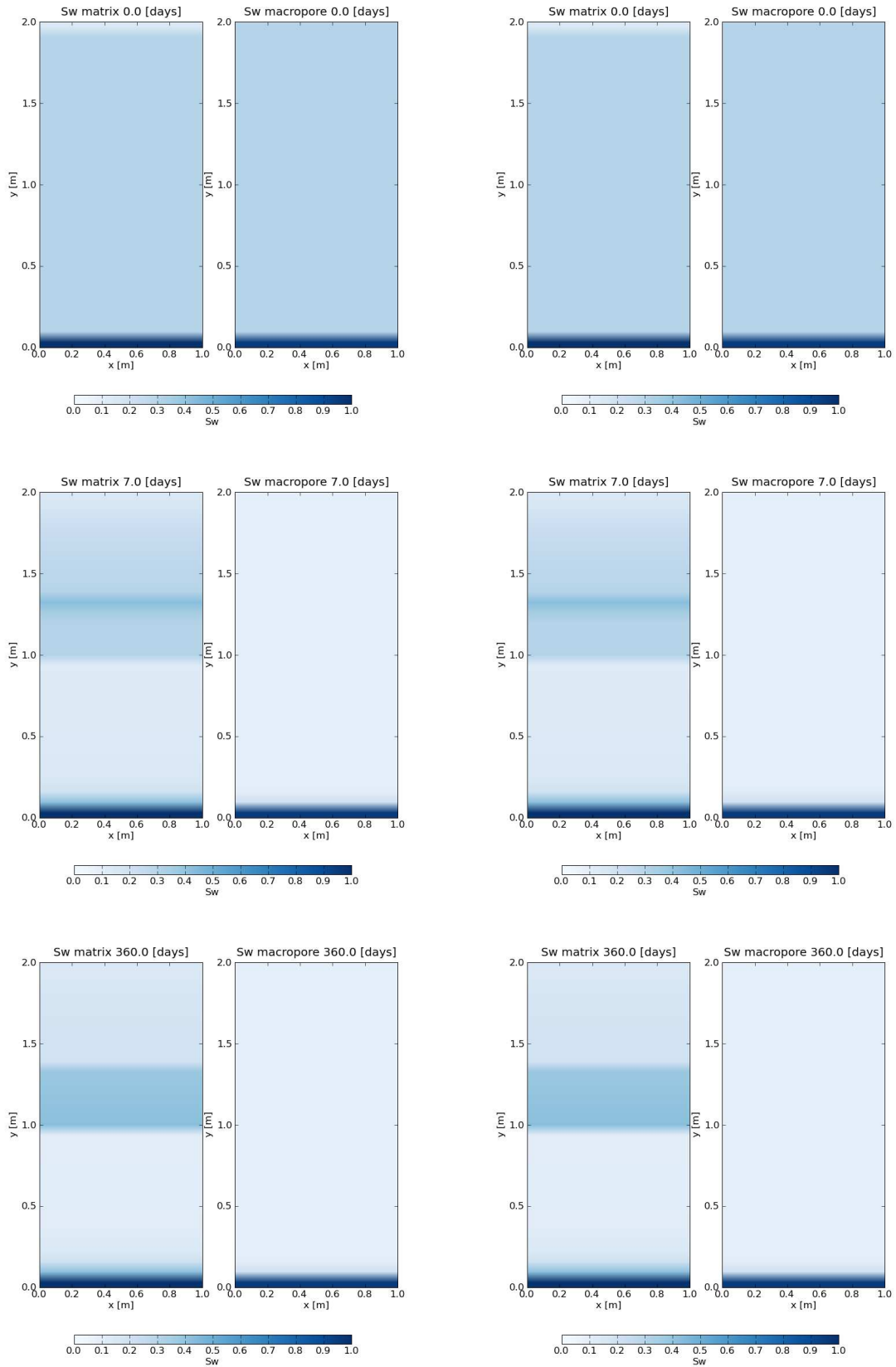
6.1.2 Results

In the lower layer, water flows downwards due to high permeability and dominating gravity. This also occurs in the upper layer, but to a lower degree, according to the association of permeability values. In the medium layer, on the contrary, water inflowing from above piles up on top and flows slowly downwards, until finally it is spread in this layer and held due to capillary forces.

Macropores, on the other hand, let the whole quantity of water pass through them, until they keep only their residual saturation. Slight exchanges are also observed in the whole duration of the simulation between macropores and matrix, especially towards the medium layer, which is the least permeable. The above can be observed in the following images from two simulations, where the domain is shown as a two-dimensional column. Case a) refers to harmonic averages for beta permeabilities, while b) to lower values than the ones of the layers.

As conclusions,

- water saturation curve follows the saturation curve form under capillary forces, but taking into account the different layers. This was expected, since at the final steady state, water capillary forces are the ones holding the remaining water in the pores.
- saturation, indicating capillarity, is as higher as smaller the size of the pores is or equally as higher the porosity is. This means that ground formations with high total pore volume, but irregular, open grain structure [Kavvas, 2005], as the clay layer, imbibe water to their fine pores. On the contrary, ground parts with large pore diameters and no cohesion, as the macropores, do not display high capillary forces.
- capillarity is though to be observed also at the macropores in a low degree, as water exists in the end a little above bottom aquifer level.
- Finally, the application of different beta parameters results in almost identical saturation curves, which was expected, as steady states were to be reached. They also play not such an important role in the intermediate states, but simply help the time development vary slightly.



(a) β : harmonic averages

(b) β : lower than layer permeability

Figure 6.1: Steady State simulation

As a consequence of the last conclusion, an arbitrary image of the fortieth-second day was chosen among the produced curves as an initial condition for the next calculations (see figure 5.4). This is regarded as a sufficient choice, since there were no spectacular differences between the various curves, and the infiltration has developed in the largest part within this period.

7 Infiltration with Dirichlet and Neumann Boundary Conditions

Two of the most commonly used boundary conditions in the continuity equation are the Dirichlet and the Neumann BCs. Their influence on the infiltration process must represent the physical conditions and processes, and therefore their role to water infiltration is examined and compared in the present chapter.

7.1 Dirichlet BC Simulation

A Dirichlet BC is used to set a constant value of either saturation or pressure. Specifically, in the formulation of water saturation-air pressure $S_w - p_n$ applied here, it can refer to either saturation of water or pressure of air. At the top boundary, where the different boundary conditions are tested, an air Dirichlet BC is always applied, as already mentioned, in order to ensure that the top surface of the domain is a free surface and not under a water layer. A water Dirichlet BC, setting a constant water saturation value, indicates a certain part of the pores which is filled with water during infiltration.

7.1.1 Setup

The exchange parameters β are chosen equal to the harmonic averages of matrix and macropores for each layer. Water saturation on top is set at 30% and 70% in two different calculations in the double-continuum model, as in figure 7.1.

The calculation covered a period of one year, images are though displayed only until a steady state is approached.

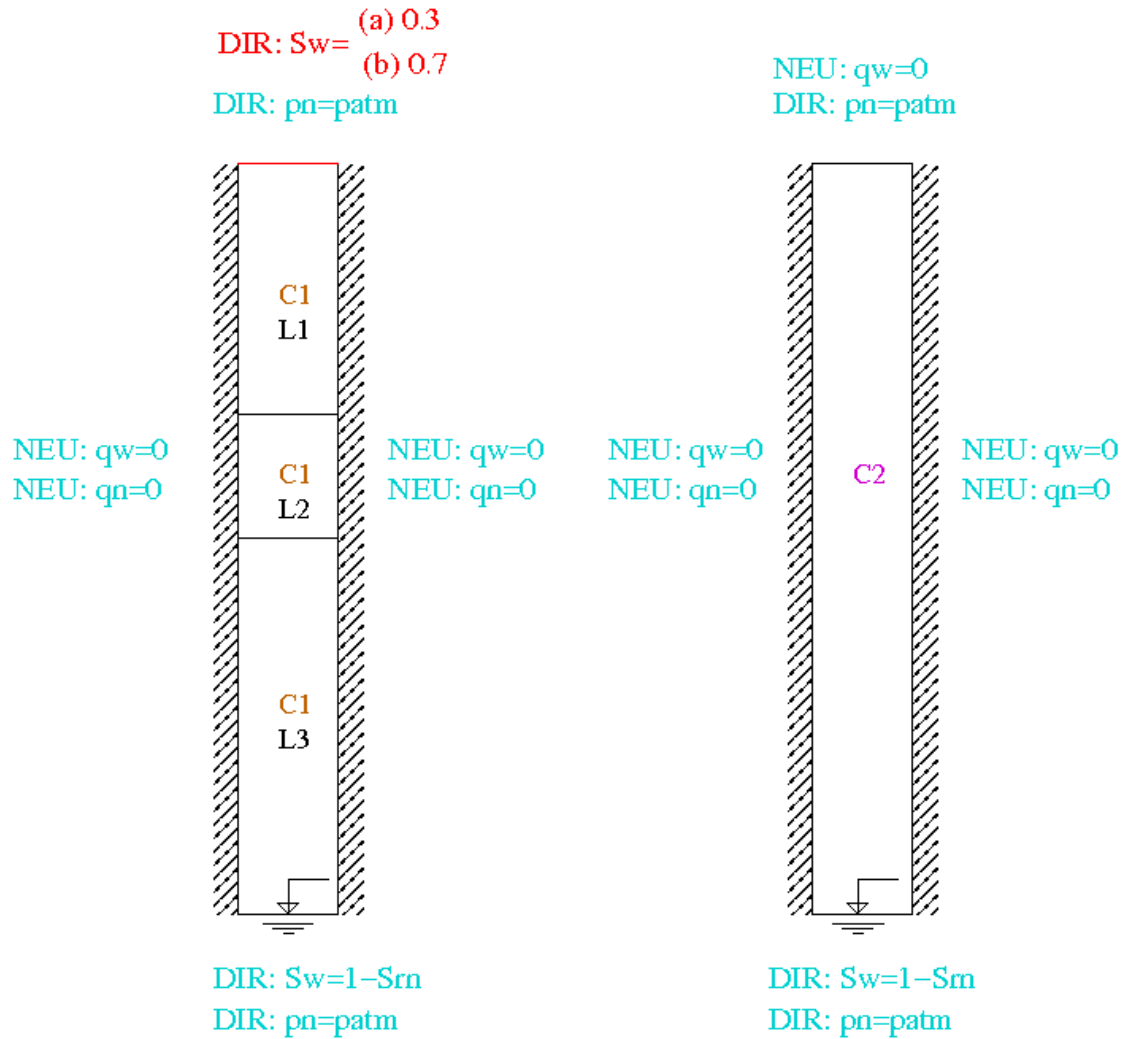


Figure 7.1: Boundary conditions for the Dirichlet simulations

7.1.2 Results

As soon as infiltration begins into the upper layer of the porous matrix, exchange is to be observed with the macropores. While then water flows through the macropores, it is again absorbed by the porous matrix at lower points, where water has not yet been infiltrated from above ((a)day 7, (b)day 1). When it reaches the clay layer it has to be piled up on the higher part, until pressure is large enough to let it flow further downwards ((a)day 21, (b)day 2). Finally water fills the medium layer and afterwards also the lower one ((a)day 63, (b)day 4).

Although the form of the saturation curve is the same in both cases of low and high

saturation at the top boundary, differences can be observed. In specific, in the first case, a pick is formed at the bottom of the clay layer, while in the second one, the curve is more smooth in this layer, with the highest saturation value in the middle of it. This could possibly be due to variability of the mobility of water at that point in the two cases. A satisfactory explanation could be given if considering the capillarity in both cases, depending on the saturation (see section 3.3.3). In the case of low saturation at the top boundary, the medium layer has apparently low enough saturation, so that it absorbs water from the layer below. On the contrary, it is much more filled in the second case, so that capillary forces are not dominant.

Profiles of the saturation describing the entire procedure are presented in the following. They are cross sections to the two-dimensional column presented previously, where the blue curve stands for the matrix and the green one for the macropores.

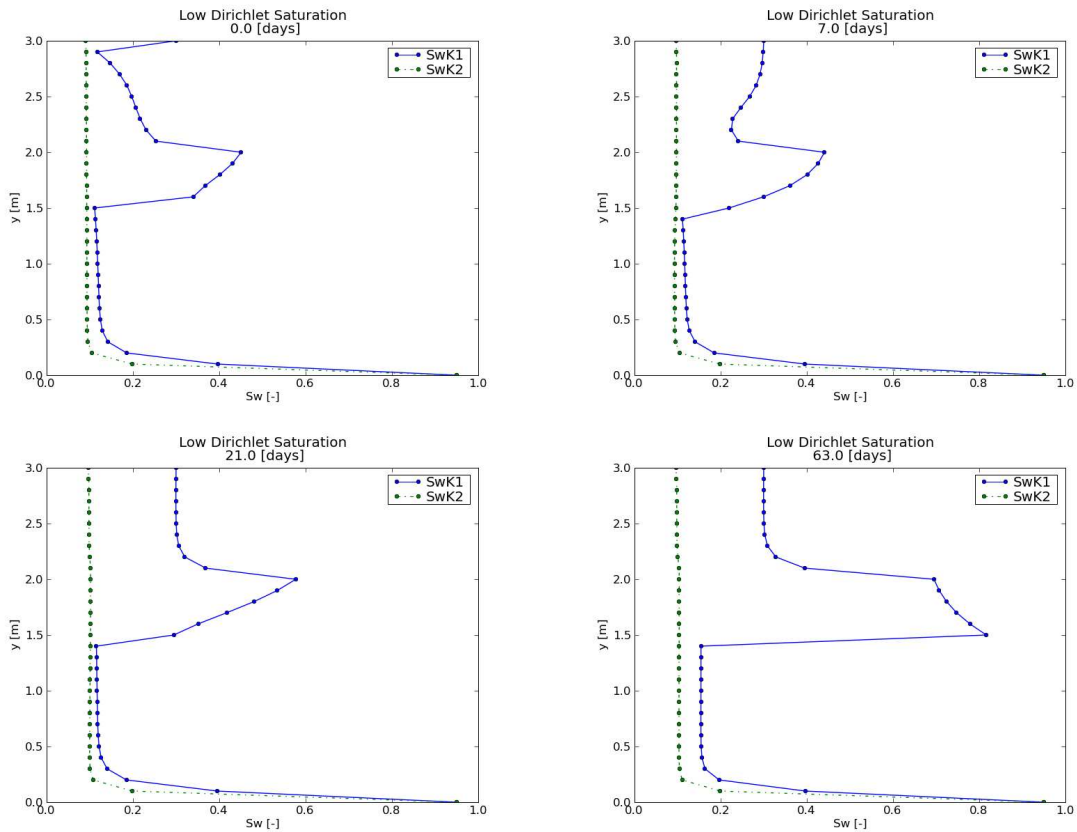


Figure 7.2: Dirichlet Simulation: (a) 30% saturation at matrix top boundary

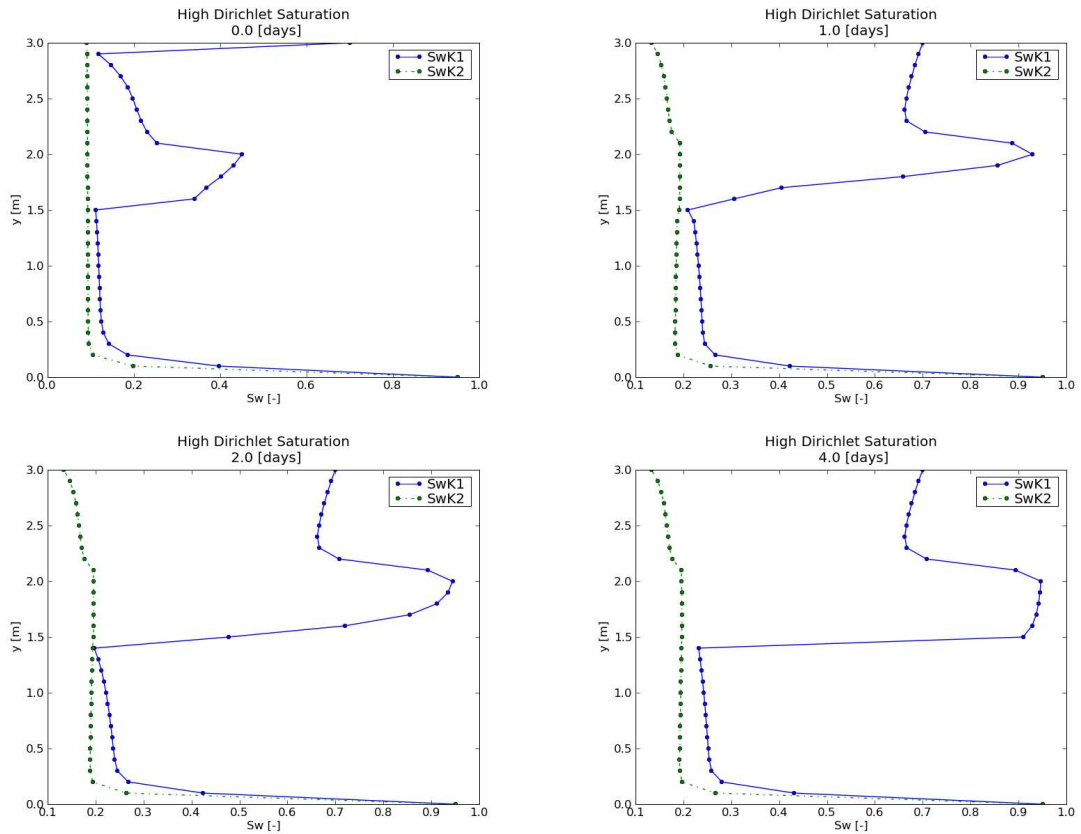


Figure 7.3: Dirichlet Simulation: (b) 70% saturation at matrix top boundary

7.2 Neumann BC Simulation

A Neumann BC is applied in the case of a certain flow value, for either water or air, given in terms of mass flux. At the top boundary, the water boundary condition for the macropores is always set at zero inflow, which implies that water always infiltrates first into the pores because of their larger capillary forces. A constant water flow on top of the matrix can represent for example a simplified rainfall event or a steady water supply on the surface for agricultural purposes.

7.2.1 Setup

The model properties are set as previously. The infiltrating flow is set in the first calculation presented here equal to a lower one, namely corresponding to an intensity of 0.36mm per hour, while in the second one equal to 36mm per hour, a hundred times

higher one. The setup of the boundary conditions at the domain is given in figure 7.4.

This simulation's duration is also one year and images of the saturation are displayed in time points figuring the development of the infiltration.

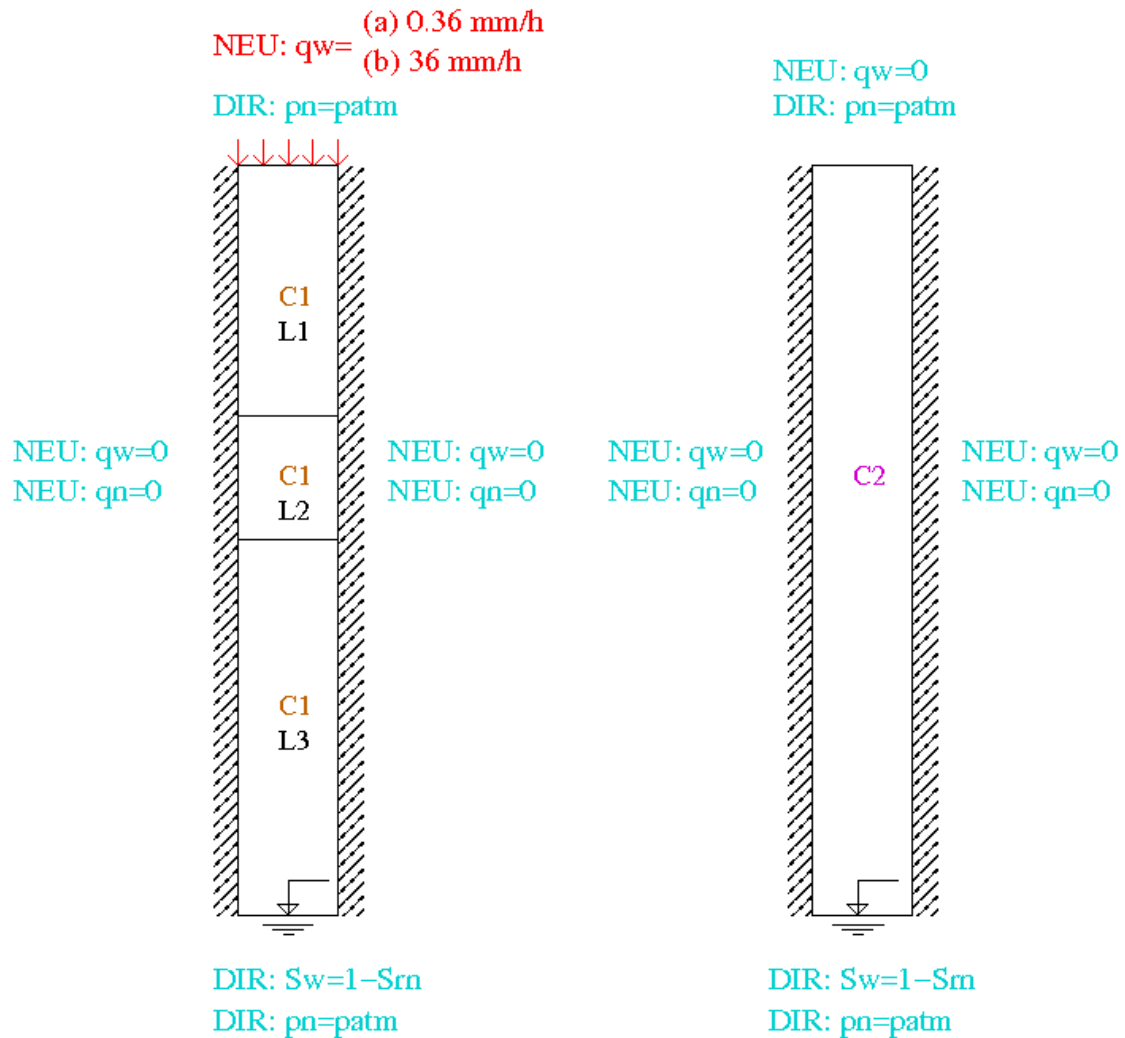


Figure 7.4: Boundary conditions for the Neumann simulations

7.2.2 Results

An intense activity of the macropores is observed. Water flowing into macropores from the pores of the matrix in the upper layer ((a)day 3, (b)day 0.1) is later on absorbed by the clay layer and the gravel ((a)day 15, (b)day 0.4), whereas when infiltration water from the loamy sand reaches the lower layers, macropores also receive water back from

them((a)day 28, (b)day 1.7).

An important point concluding from the simulation results is that the water exchange between macropores and matrix is clearly more significant in the high inflow simulation, allowing macropores to reach higher saturation degrees.

Another outstanding aspect is the different slope of the saturation curve in the gravel layer in the final state for the two simulations. While in the lower infiltration rate case it is vertical, in the second case it obtains lower values on top of the layer. This could possibly be explained by the fact that in the second simulation the medium least permeable layer is much more saturated than in the first one, and therefore capillarity is smaller than in the first case.

These can be observed in the following figures, which have been chosen according to the most characteristic phases of the infiltration development in the two cases.

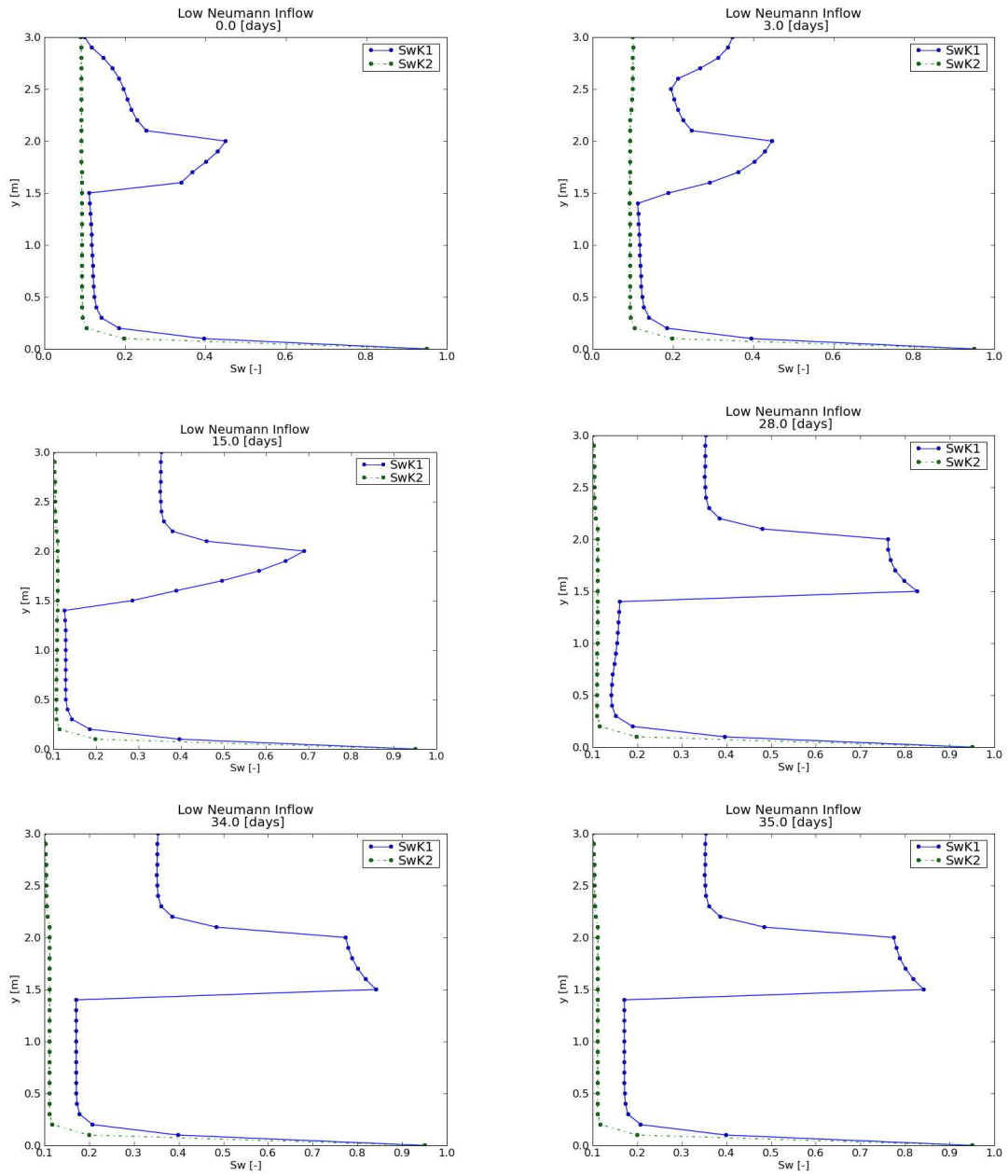


Figure 7.5: Neumann simulation: $0.36 \frac{\text{mm}}{\text{h}}$ at matrix top boundary

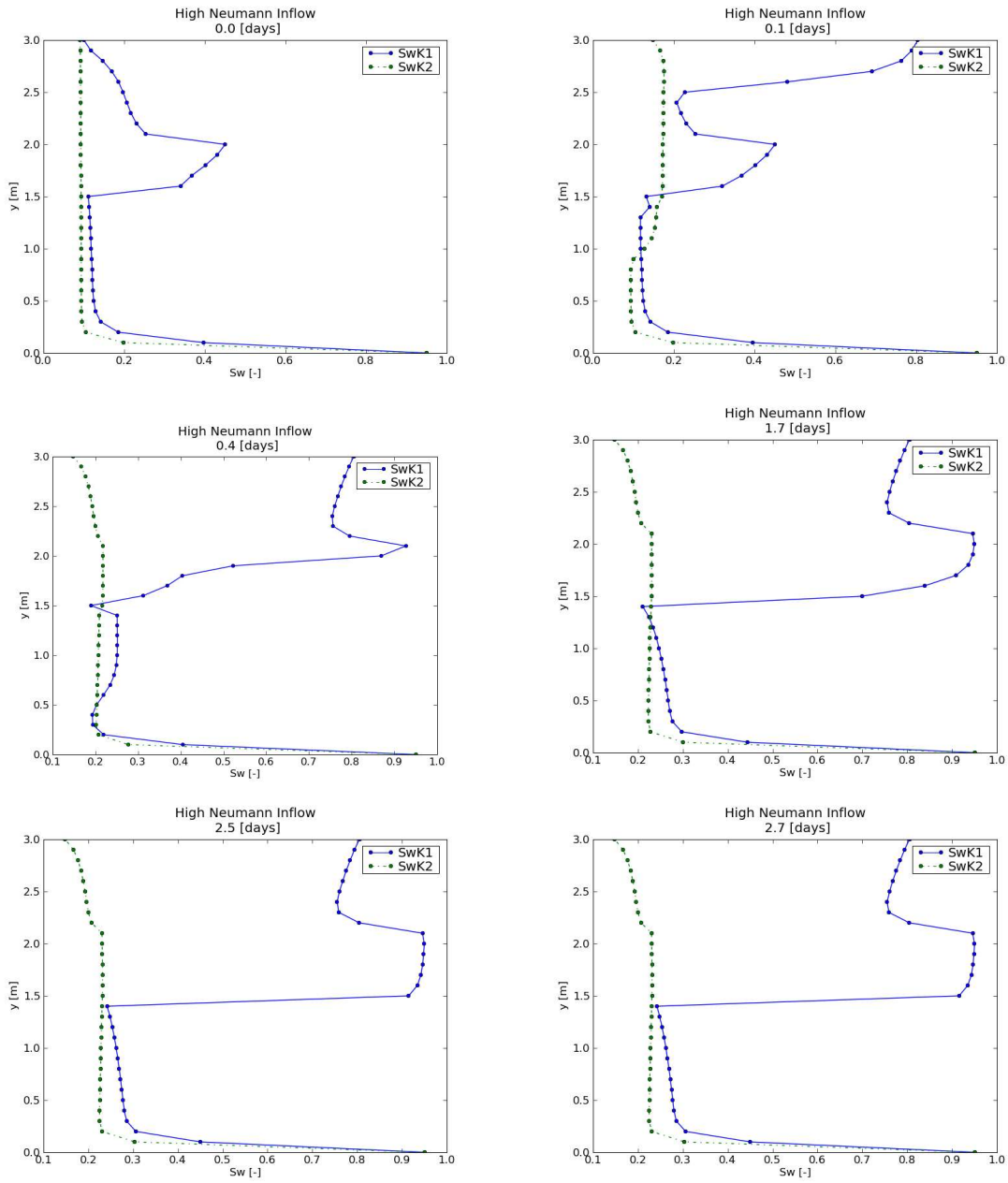


Figure 7.6: Neumann simulation: $36 \frac{mm}{h}$ at matrix top boundary

7.3 Comparison

There is no strictly defined basis on which the Dirichlet and Neumann calculations presented above can be compared. The saturation of the first simulation on top can not

be converted into a flow quantity for the second simulation. In spite of this, remarks on the way of function of the two different boundary conditions, regarding the final state reached, can be made:

- The saturation curves have the same form, as was expected since the final solution of the partial equation is independant on the boundary condition type.
- The saturation of the lower layer decreases more with the height in the Neumann model than in the Dirichlet one.
- Water piles up above the medium layer slightly more intensively in the Neumann than in the Dirichlet simulation.

8 Infiltration with Rainfall Boundary Condition

None of the boundary conditions discussed above can represent physical reality accurately, not even be absolutely appropriate for certain types of problems. For example, a Dirichlet BC ensures a constant saturation value, something that could be defined by measurements, but the mass flow cannot be known. As a result, water may be calculated as flowing in larger amounts than available. On the other hand, a Neumann BC provides the calculation with a flow quantity through ground surface, but the flow values in the cells are not known.

This leads to the need for forming a new boundary condition, combining the concept of the two already used ones. A flow value is thereby set as input at the boundary, which is distributed to porous matrix and macropores, depending on their potential to infiltrate water. Details are supplied in the following section.

8.1 Implementing a Rainfall Boundary Condition

The suggested 'Rainfall' BC describes a concept for infiltration of a water quantity on the surface, which could origin for example from a rainfall event, with no steady and a priori known inflow values. In this case, water on surface flows into the porous matrix first, if the difference of the hydraulic potential between above surface and underneath is adequate. In other words, adequate pressure difference between these points, in combination with gravity, are required. Another point of view is the capillarity near the surface. The higher the capillary forces, the easier water is imbibed into the matrix. As the matrix pores are filled with more water, its water saturation grows. Above a very high saturation, near to one, water cannot physically fit into the pores of the matrix and therefore it flows into the macropores, as long as there is respectively hydraulic potential between surface and macropores. Then the same concept is adopted for the flow into the macropores. When the macropores are also filled, the rest of the rainwater reaching surface leaves the domain as surface flow.

8.1.1 Modelling the Rainfall BC

This boundary condition, as explained above, is based on the idea that water exchange between ground surface and domain occurs according to the piezometric head gradient and that infiltration requires available space in the pores. Implemented quantities and assumptions needed for the controls in the boundary condition, based on previous works of *Mieth* [2008], are described next and presented in a simplified visualisation example in figure 8.1.

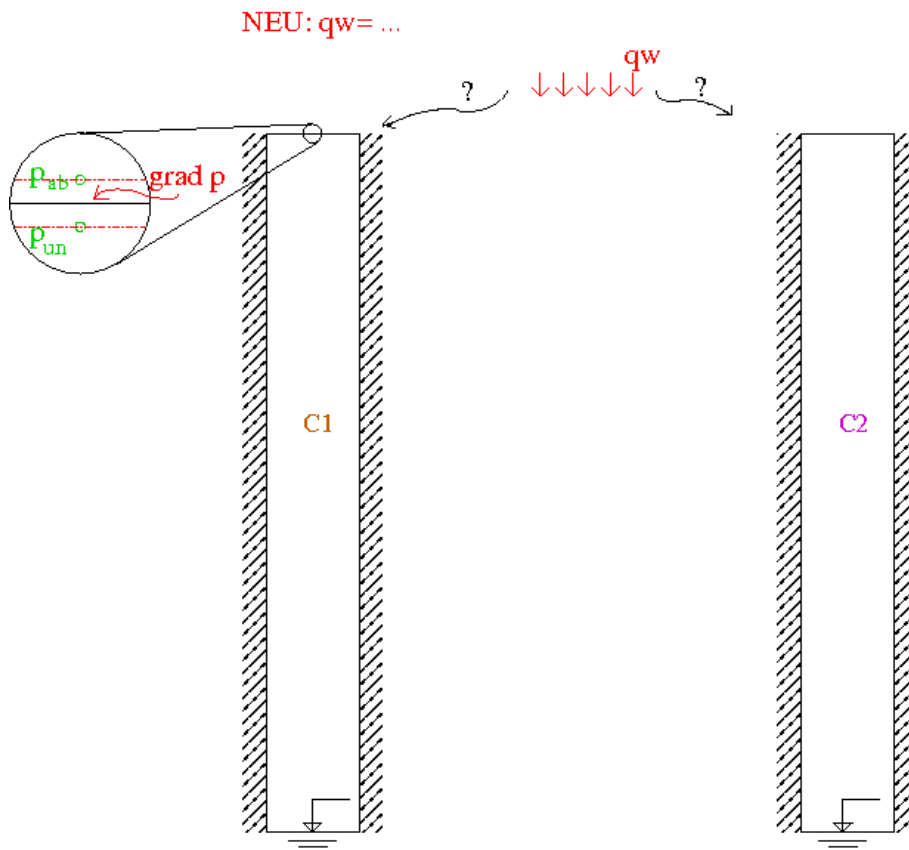


Figure 8.1: Rainfall boundary condition on top of the domain

8.1.1.1 Implemented Quantities

The difference of the piezometric head between above surface and underneath, is expressed for each continuum by the difference δh_m and δh_p , generally reading to

$$\delta h = h_{ab} - h_{un}. \quad (8.1)$$

Regarding the expression of the piezometric head, defined in equation 3.16, the difference is formed as

$$\delta h = \delta p_w - \rho g l_{grad}. \quad (8.2)$$

By use of this formulation, a difference of water pressure values is managed to be required,

$$\delta p_w = p_{w,ab} - p_{w,un}, \quad (8.3)$$

where the values are known. Specifically, water pressure above surface $p_{w,ab}$ is assumed equal to the pressure of an extremely thin water layer of width $z_r=1\text{mm}$, so that free surface is maintained, and reads to

$$p_{w,ab} = p_{atm} + \rho g z. \quad (8.4)$$

Water pressure exactly beneath $p_{w,un}$ is derived from the upper cells from the previous calculating time step by the existing MUFTE-UG.

The problem arising at adopting this pressure difference concept is that the surface is a plain with no width, so that the points on either side are actually identical. On the one hand, pressure is a continuous quantity, where jumps are not allowed at one point, but on the other a pressure difference practically at the same point is assumed, so that flow exists. In order to overcome this obstacle, a distance between these two points is assumed, which results in a pressure gradient when dividing δp_w , the required by the Darcy law gradient. The implemented length between the two points l_{grad} is arbitrary and considered equal to 0.5mm .

The rainwater flow Q_r is expressed in mass per time unit and is given in the present as a time function. The water flow that the pores of the matrix, or respectively the macropores, can potentially infiltrate, in terms of mass per time unit, is expressed for each continuum as

$$Q_{pot} = v A, \quad (8.5)$$

where

$$v = \frac{k_{rw}}{\mu_w} k_{grad} \delta h. \quad (8.6)$$

In this formulation of the Darcy velocity, a permeability term which includes the length

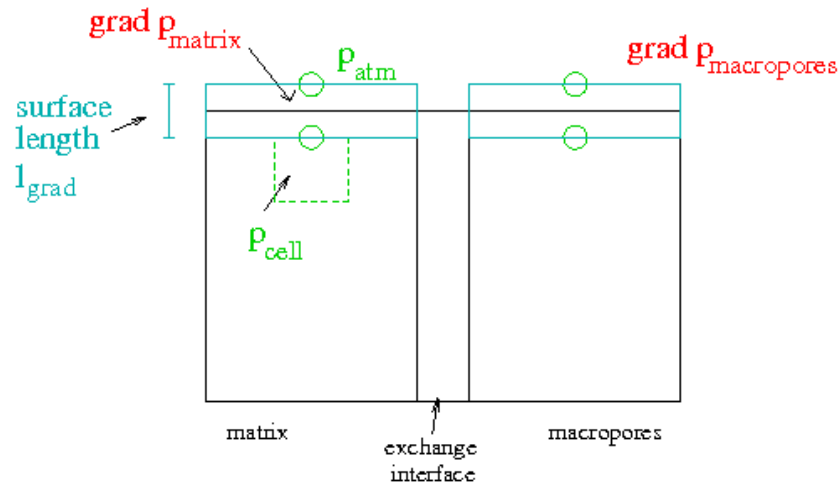


Figure 8.2: Implemented surface length and pressure gradient

l_{grad} is introduced, namely

$$k_{grad} = \frac{k}{l_{grad}}. \quad (8.7)$$

This modification of the permeability indicates a connection of the length l_{grad} to the absolute permeability k , and therefore values of k_{grad} can be examined instead of arbitrary values for l_{grad} .

8.1.1.2 Structure of the Boundary Condition

According to the adopted concept of the Rainfall BC, two controls take place:

1. The sign of the piezometric head difference determines the direction of water exchange between surface and the domain. Positive values of the piezometric head difference refer to inflow, so if $\Delta h > 0$, water is infiltrated, as long as criterion 2 is also satisfied. At negative values, $\Delta h < 0$, the same control is held respectively for the macropores. If it is not fulfilled, water counts as surface flow (see assumption 4). For values around zero, there has been no special formation of the condition, but the same control for the macropores is assumed for $\Delta h = 0$.
2. The mass flow on the surface is compared to how much water can potentially inflow into the domain, first into the pores of the matrix, the rest into the macropores and the rest of it is rejected. So, at a positive piezometric head gradient Δh , if $Q_r < Q_{pot}$ for the matrix, all of the water can be infiltrated into the pores. If

$Q_r > Q_{pot}$ for the matrix, the same control takes place for the macropores, namely if $Q_r < Q_{pot,mat} + Q_{pot,por}$, the water quantity over the potential of the matrix, infiltrates into the macropores. If $Q_r > Q_{pot,mat} + Q_{pot,por}$, the extra quantity flows away.

This concept is visualised in figure 8.3.

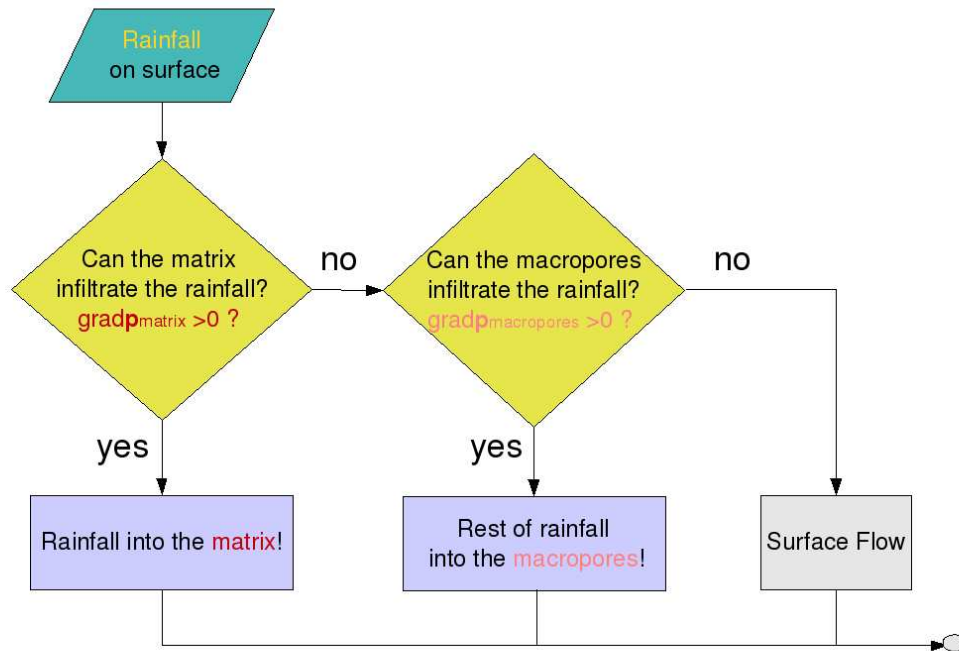


Figure 8.3: Flowchart for the Rainfall BC concept

Precipitation Q_r is implemented here as either constant or varying flow value. It can though be further developed, to an input at a time series of rainfall measurements or even to a randomly produced rainfall event, implementations which are beyond time limits of the present thesis.

8.1.1.3 Assumptions

The present application is based on certain assumptions :

1. There is a distance between the points above and underneath the surface of the domain, as explained in section 8.1.1.1. This length l_{grad} is no physical quantity

and therefore assumptions have to be made, since experiments do not cover yet this issue . It is considered to depend on the magnitude order of the domain or also the hydraulic properties of the ground, and therefore the permeability k_{grad} could be easier to study in the future through simulations or better laboratory experiments.

2. The relative permeability k_{rw} used in the form of water velocity is calculated by the Van Genuchten relation, except for the case of positive piezometric head gradient for the matrix. In this case, the relative permeability is considered equal to one , $k_{rw} = 1$, so that an infiltration first into the porous matrix is ensured. Physically, this can be accepted, since the fine pores of the matrix near the surface absorb water before macropores do, due to stronger capillarity, and so the upper points, or in the simulator the upper cells, have locally a larger saturation than the average of the matrix and therefore a high relative permeability.
3. As already mentioned, water is modeled to infiltrate first into the matrix. The infiltrated water is assumed to fill the whole of the pores before it also flows into the macropores. This means that exchange between matrix and macropores as far as incoming rainwater is concerned are neglected. Such exchange is still described by the existing MUFTE-UG, through the interface A_{il} .
4. At a negative gradient Δh where also the macropores are completely filled with water, case which represents exfiltration, an additional control is held. The relative permeability of the matrix water has to be positive, $k_{rw} > 0$, so that it is ensured that water exists and can indeed exfiltrate. A different case could occur, if for some reason the pressure gradient were positive , but the pores of the matrix empty. This safety control indicates a fully upwinding process, namely that water flow occurs on the direction of the gradient only at non-negative relative permeability k_{rw} , or respectively positive mobility λ .
5. Water that does not infiltrate is not further dealt with, as it is considered as surface flow, not affecting the domain. To this assumption, inclination of the surface could be considered macroscopically, although the domain is formed with a horizontal top surface, as described in section 5.2.1.

8.1.2 Relation to existing Boundary Conditions

According to the previously mentioned, a Rainfall BC can selectively act as rather a Neumann or a Dirichlet BC. When water infiltrates into the porous matrix, a mass flow

value is given as a boundary value, which is close to a Neumann BC for the matrix. If , on the other hand, matrix pores are full and water infiltrates also into the macropores, a saturation value is practically steady for the matrix, which is similar to a Dirichlet BC, and a mass flow value is applied to the macropores boundary, which represents a Neumann like BC. If finally, water fills pores and macropores, two saturation values are set at the boundaries, so we could assume the function of a Dirichlet type for both continua.

In all cases, the distribution of the flow into matrix and macropores is known, in contrary to Neumann and Dirichlet BC. This allows control of the functional part of the simulating software and further study of the mechanisms of infiltration into the two continua.

8.2 Input from a Rainfall Event

A factor which is not applied in the previous simulations is the variability of the values of flow that reaches surface. During a rainfall event, or even in a larger period with more rainfall events, flow values on the surface are not constant, but may change dramatically and in various time spaces. The sequence of irregular events causes complex images of water infiltration, especially when the influence of the macropores is also taken into account. Such an event was simulated applying a Rainfall BC.

8.2.1 Setup

The domain geometry and properties are identical with the ones used up to now.

The Rainfall BC was formed as a time function. Arbitrary values of precipitation were applied for discontinuous random periods, assumed constant during the events, for sake of result simplicity. The implicated event is described in table 8.1 and in figure 8.4.

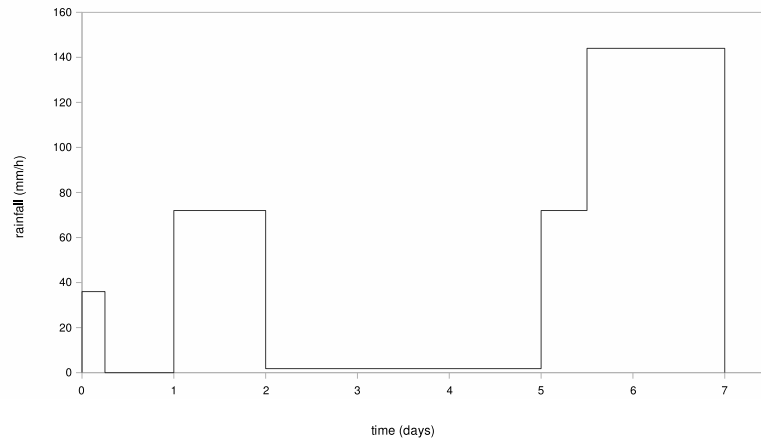


Figure 8.4: Development of the applied rainfall event

time (h)	0	6	24	48	120	132
rainfall intensity (cm/h)	3.6	0	7.2	0.18	7.2	14.4

Table 8.1: Rainfall event inflow values

The time scale is defined by the chosen values for the sub-periods of the event. A rather short period was applied in total, namely that of one week.

8.2.2 Results

The reaction of the domain to the various flow values can clearly be displayed in the following images, which depict the most important instants of the infiltration development. More specifically, three periods of the entire event are distinguished and presented in the respective figures:

1. the first sub-event (0-6 hours) and an interruption of its development (6-23 hours)
2. the second sub-event (24-47 hours) and a much smaller following sub-event (48-119 hours)
3. the third sub-event (120-131 hours), followed by an even more intense sub-event, the fourth one (132-168 hours).

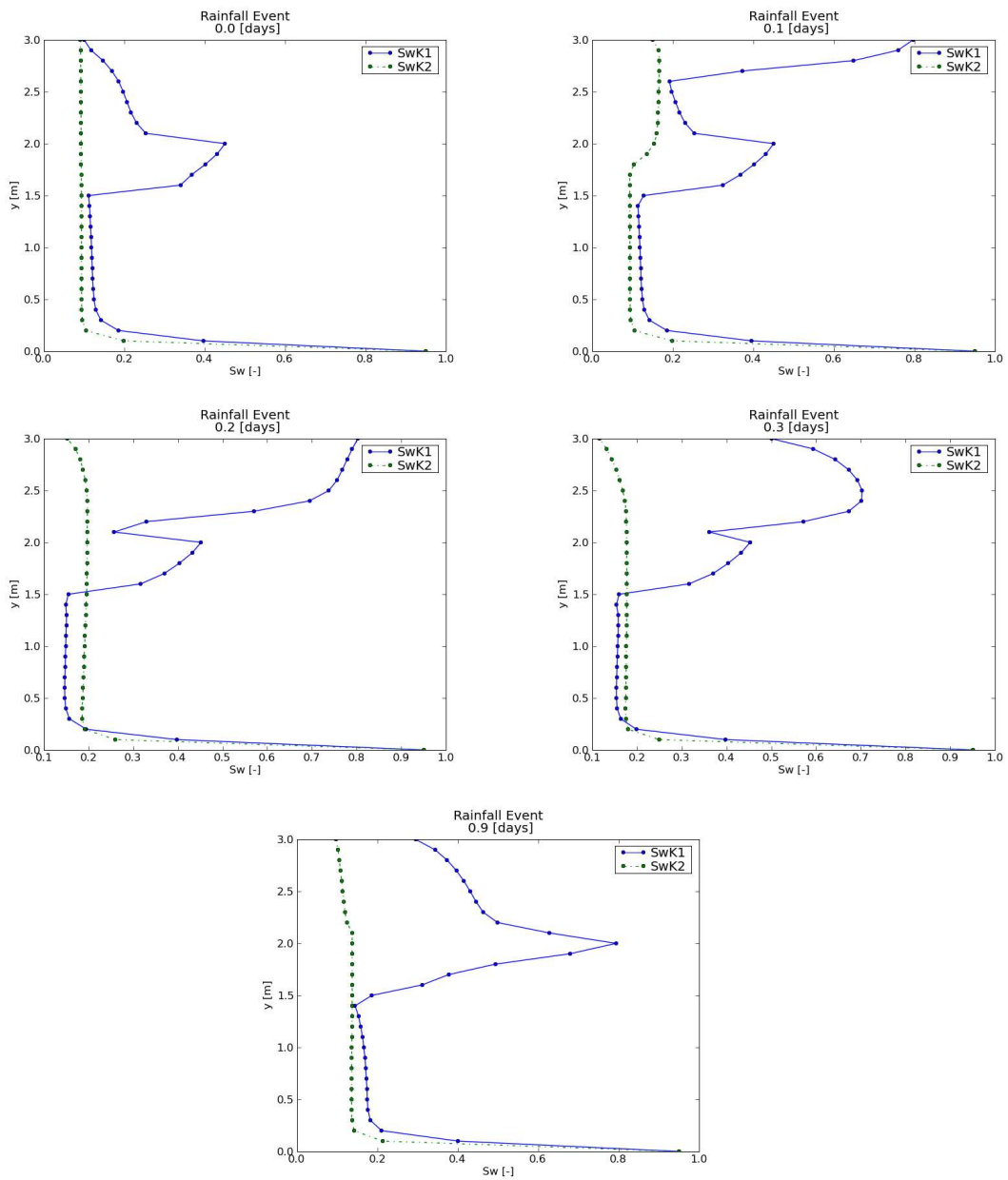


Figure 8.5: Rainfall Event : 0-23 hours

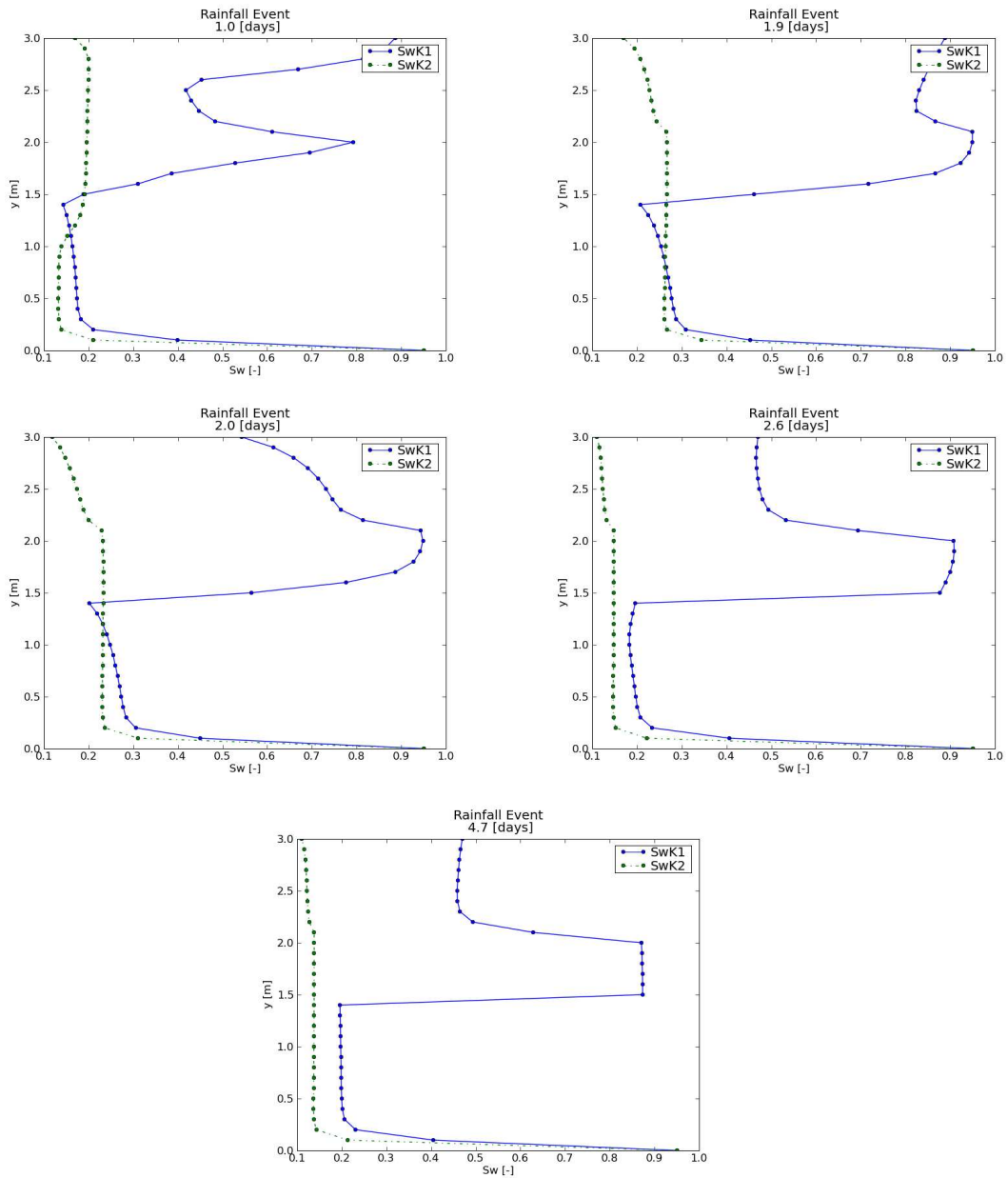


Figure 8.6: Rainfall Event : 24-119 hours

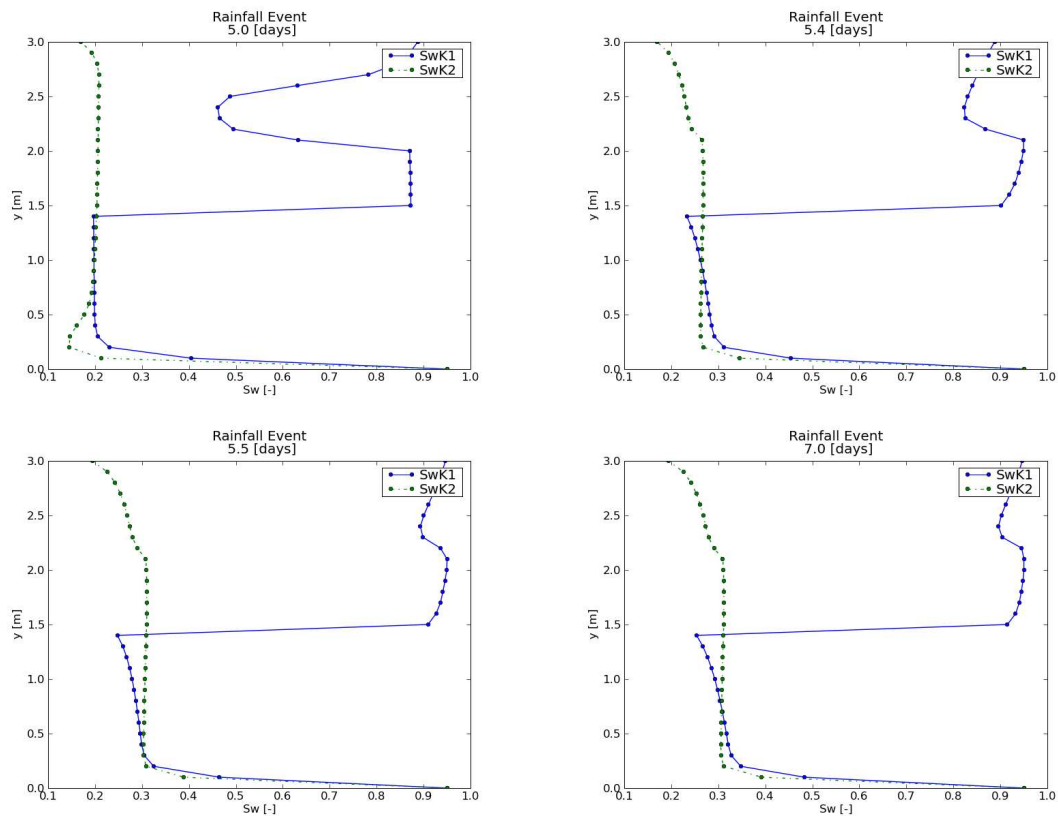


Figure 8.7: Rainfall Event : 120-168 hours

According to the previous, attention should be paid to following points:

- The flow process of infiltration which is observed in previous models remains similar in general. When the boundary condition value changes, the upper layer reacts first to this, while the medium and the lower ones continue infiltration of the water received from the previous time steps, until the 'signal' of the new condition is received. So, when a strong rainfall event is followed by a much weaker one (1.0, 2.6, 5.0, 5.5 days), the saturation is reduced beginning from the upper layer. In the opposite case (0.3, 1.0 days), the curve obtains larger values on top and later also the lower parts.
- The reaction of the domain to the sequent rainfall event is of great interest. When an intense event is followed by a more intense one (5.0 to 5.5 days), the upper layer contributes its part to the infiltration, but macropores play also a very significant role. They not only infiltrate large amounts of water, but they also conduct water

to the gravel layer of the matrix, helping it bypass the saturated less permeable clay layer.

- Exchange between pores and macropores is clear when water reaches the medium layer, where a part infiltrates laterally to the macropores(e.g. 1.2 days).

8.3 Comparing Rainfall and Neumann Boundary Conditions

A Rainfall BC actually distributes infiltrating water into pores and macropores, as said above, regulating a flux value at the boundary. A similar process could be obtained by a domain with a humus layer on top, which infiltrates water to the boundary of the matrix and macropores depending each time on their properties.

Specifically, a humus layer, consisting of organic material, such as leaves, and also ground material, such as gravel, often lays on ground surface. It is expected to have a high permeability due to rare structure. When such a layer is wet because of water flow into it, water can infiltrate through its small width onto the top of the considered ground formations. Water flows then to that formation, meaning here to matrix or macropores, which can absorb it more easily, depending on hydraulic head.

Useful observations could therefore be made by setting simulations, with different boundary conditions, one with a Rainfall and another one with a Neumann BC above the humus layer, which should though represent the same process concept. Another interesting comparison could be drawn between a Rainfall BC and a usual Neumann BC on the matrix, where the actual distributing role of the Rainfall BC could be controlled.

8.3.1 Wet Humus Layer Model

In order to describe the humus layer, uncertain assumptions were made, regarding its width, its hydraulic properties, and its distribution on top of both continua.

8.3.1.1 Setup

The width of the humus layer h_l is chosen equal to $h_l = 10\text{cm}$. It is considered to spread homogeneously on matrix and macropores. Its permeability is set slightly higher than this of the macropores, equal to $K = 5E - 9\text{m}^2$. An exchange possibility between pores and macropores also here is provided, through a positive value of the exchange parameter β of the humus layer, based on an assumed permeability $K_{il} = 1.9E - 11\text{m}^2$.

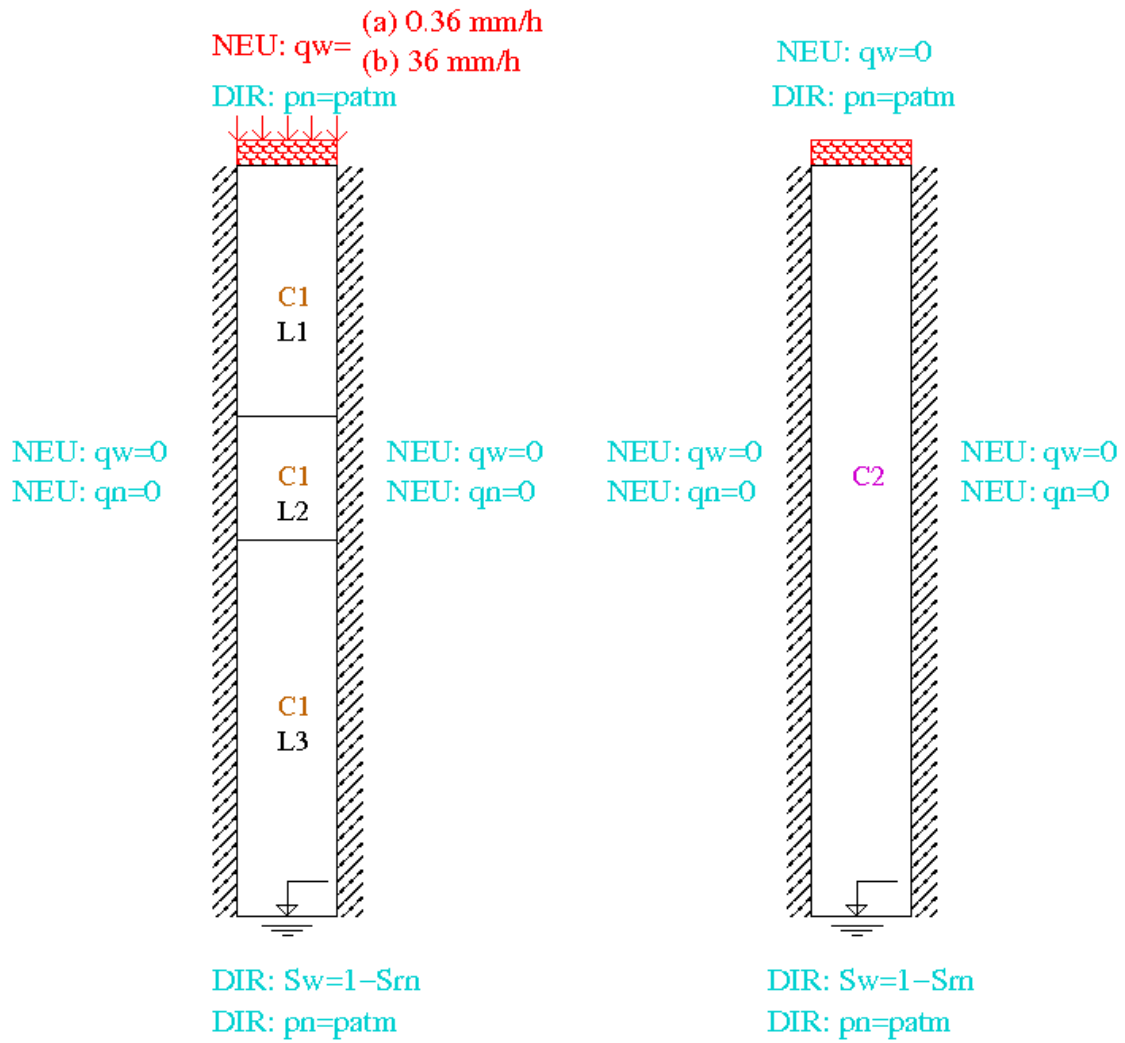


Figure 8.8: Boundary conditions for the Humus Layer simulations

The boundary condition is a Neumann BC on top of the layer. So the layer can be seen as an external adapter of the boundary condition on top of the studied domain as considered up to now. It is not constant, but dynamic, how much water will be infiltrated at the surface of the domain, meaning the interface between humus layer and main domain. There were several values of precipitation applied, while for the simulations presented here a lower value, of 0.36mm per hour, and another higher one, of 36mm per hour, were used.

8.3.1.2 Results

Water flows quickly through the macropores((a)day 3, (b)day 0.1) because of their high permeability, while in the matrix, when it reaches the medium layer, it proceeds much slower ((a)day 15, (b)day 0.4). Remarkable is the increase of the saturation in the third layer before water has infiltrated through the second one ((a)day 15, 28, (b)day 0.4, 1.7). This is a result of the exchange with the macropores. The water obtained this way is rejected downwards to the aquifer. The jump of saturation between the second and third layer is to be explained by the capillary forces imbibing water from the lower layer at their interface ((a)day 28, (b)day 1.7). Finally, when the clay is completely filled, water flows into the gravel layer((a)day 34, (b)day 2.5). A saturated steady state is then achieved((a)day 42, (b)day 3).

Figures of representative moments of the flow process are displayed in the next for both applications of the humus layer.

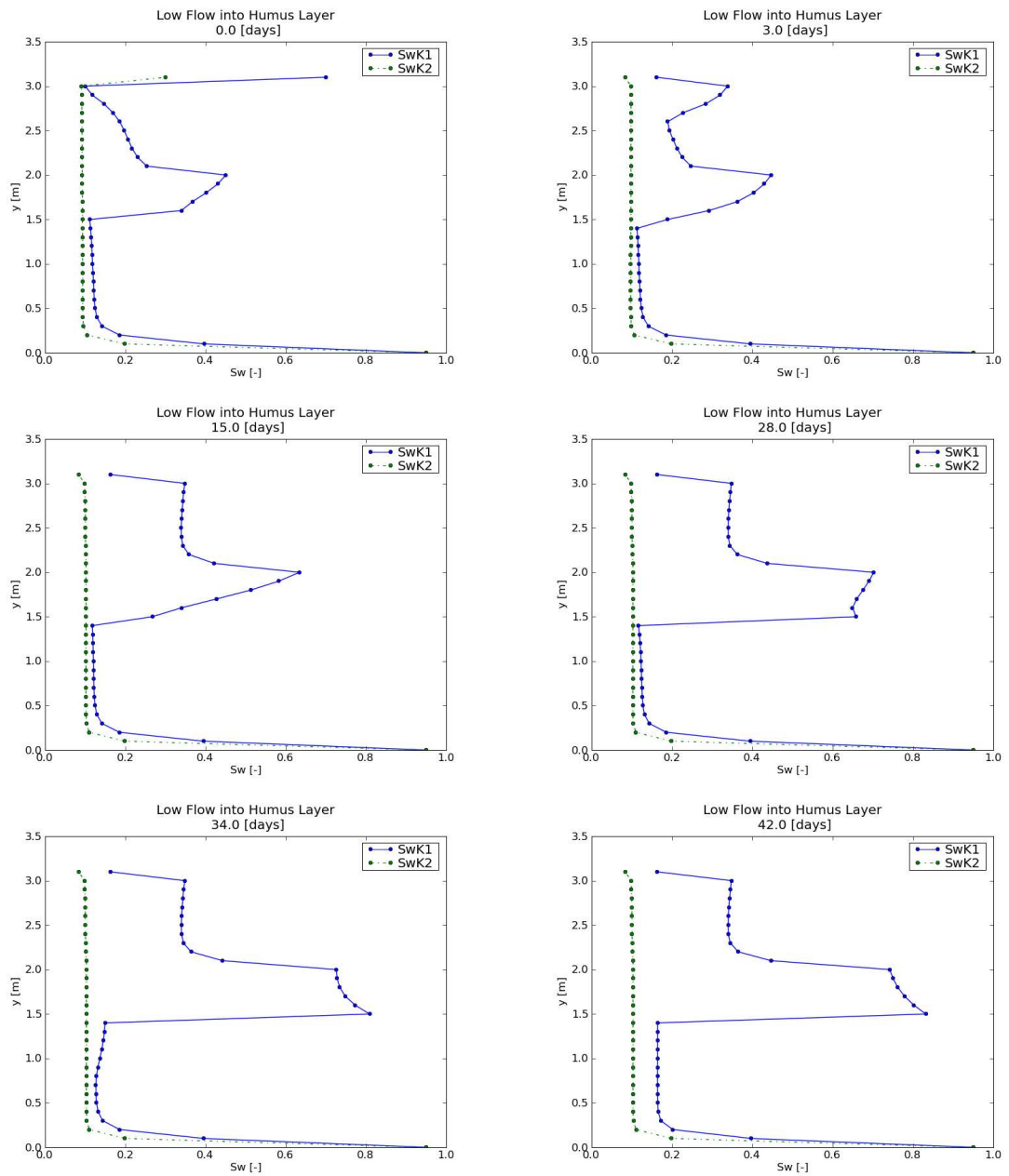


Figure 8.9: Humus Layer simulation: $0.36 \frac{mm}{h}$ at the matrix top boundary

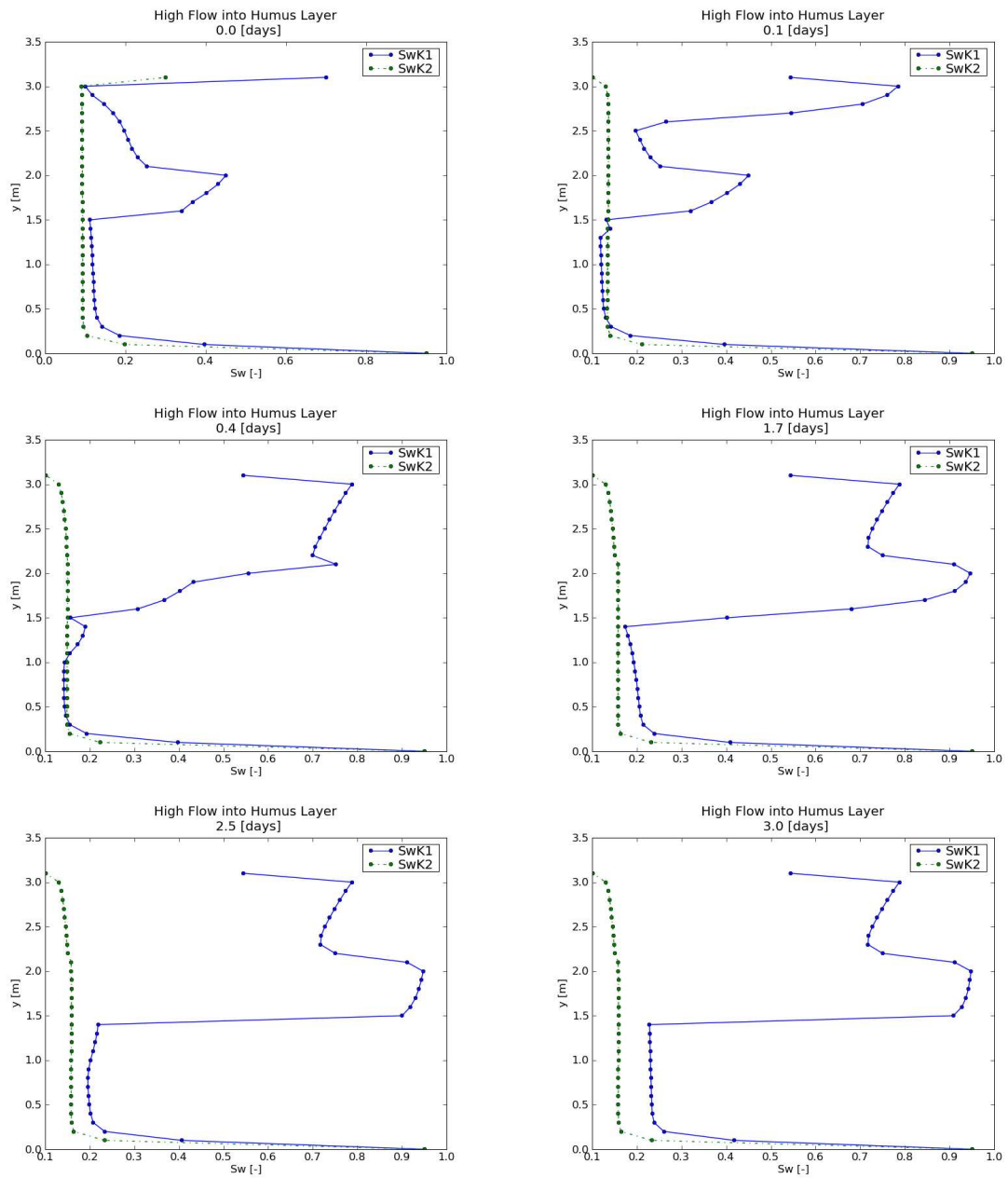


Figure 8.10: Humus Layer simulation: $36 \frac{\text{mm}}{\text{h}}$ at the matrix top boundary

8.3.2 Rainfall Event Model

In this model, the rainfall flow is considered as boundary condition directly on the surface of the domain, in an otherwise identical simulation to the previous one.

8.3.2.1 Setup

The domain, boundary conditions and duration of the simulation are the same as in section 8.2. The rainfall event was though assumed as a constant precipitation value, equal in each case to the Neumann flow value of the respective Neumann and Humus Layer model, 0.36mm and 36mm in each case, so that comparison can be drawn.

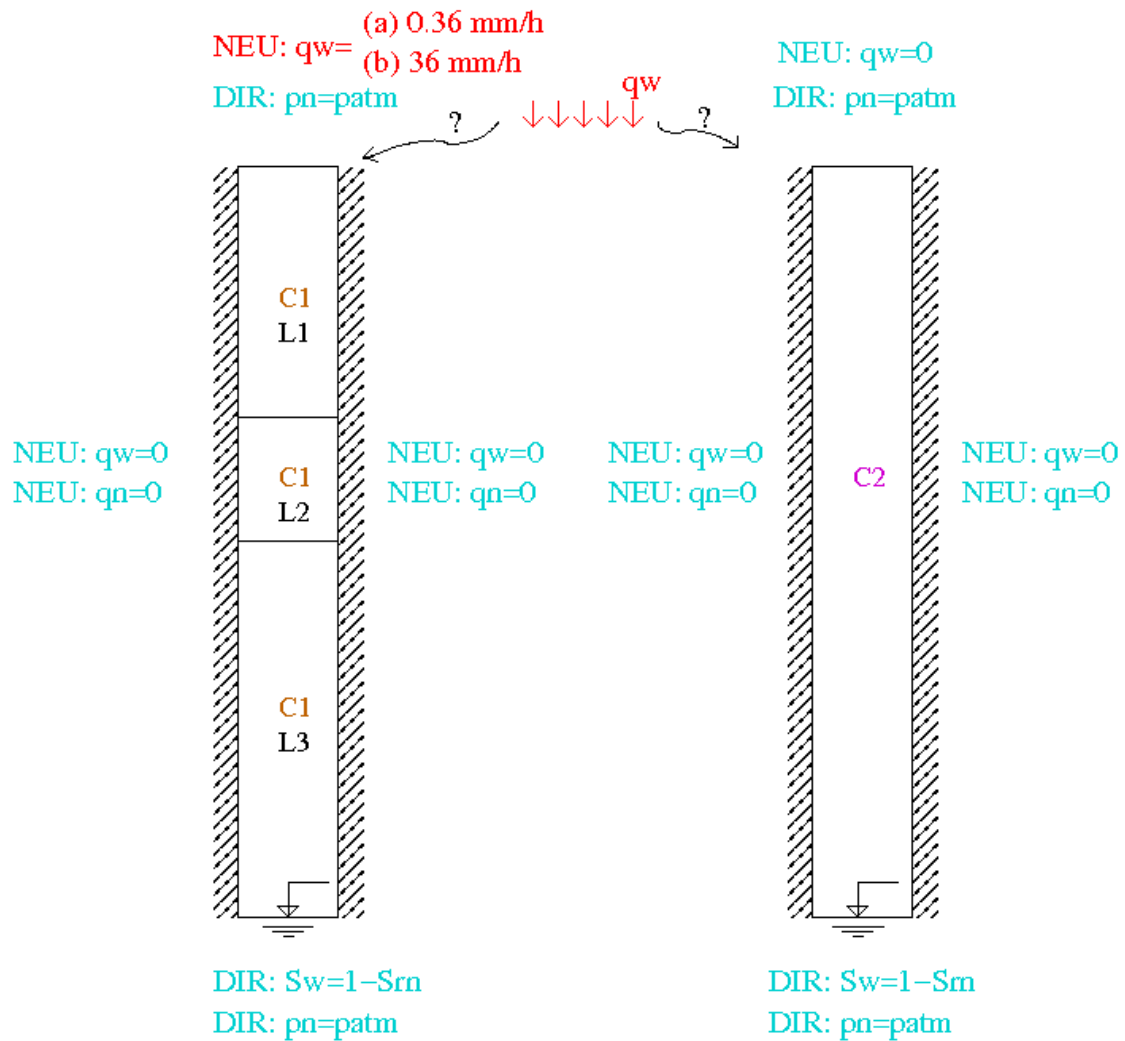


Figure 8.11: Boundary conditions for the Rainfall simulations

8.3.2.2 Results

The process of infiltration is in general the same as described in previous calculations. It should though be remarked that:

- in the simulation of high inflow, more water is infiltrated into the macropores. This shows that macropores indeed infiltrate water depending on the saturation of the matrix.
- at high inflow, water on top of the clay forms a thin layer before moving further downwards, through which it flows into the macropores. This water layer occurs because of low clay permeability and causes a higher pressure gradient towards macropores than towards the clay.

The process of the infiltration is similar to the one occurring in the Humus Layer model. Figures indicating the development of the infiltration in both cases of inflow follow, at the same instants as previously, for comparison's sake.

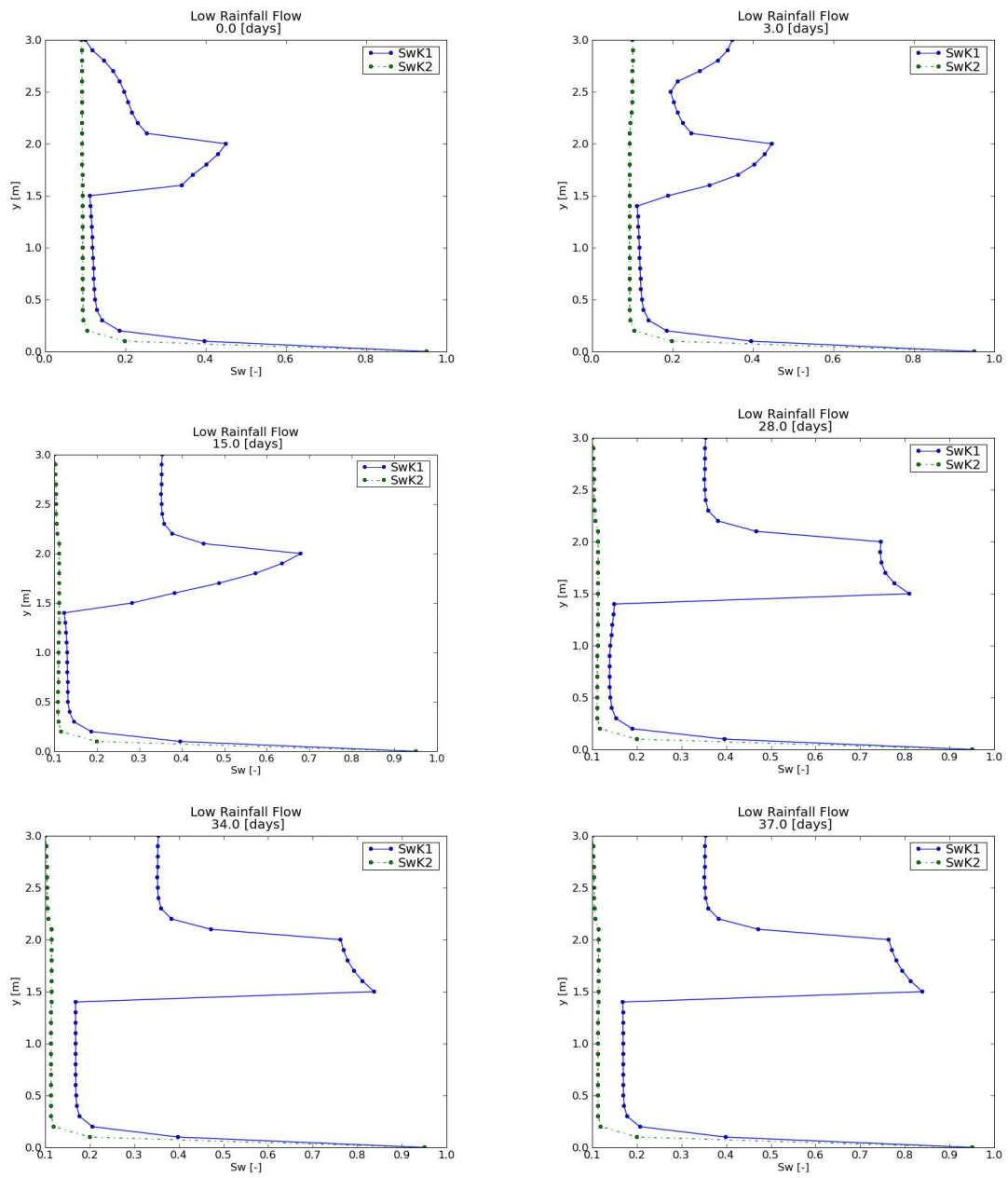


Figure 8.12: Rainfall simulation: $0.36 \frac{\text{mm}}{\text{h}}$ at the matrix top boundary

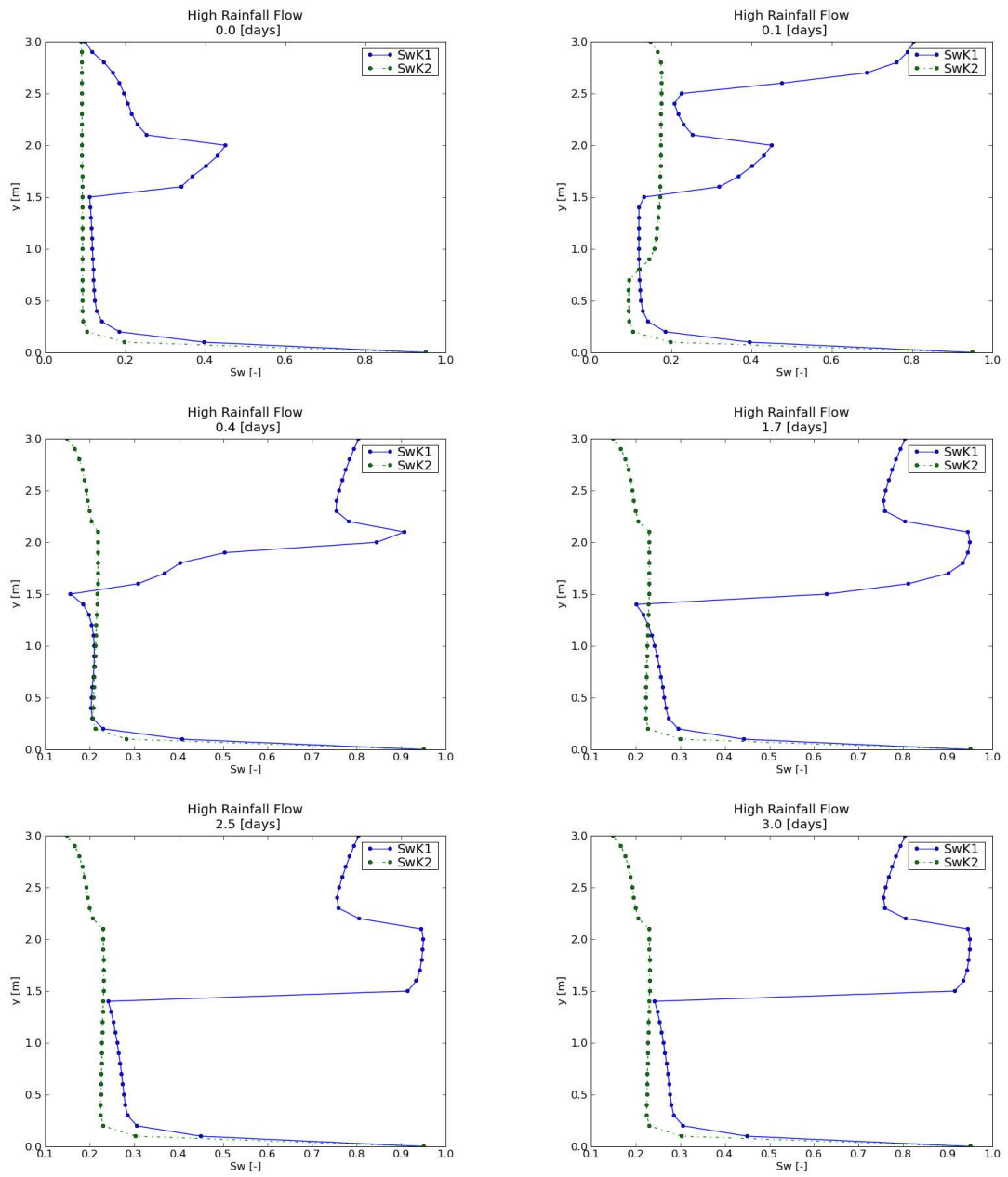


Figure 8.13: Rainfall simulation: $36 \frac{\text{mm}}{\text{h}}$ at the matrix top boundary

8.3.3 Comparison

8.3.3.1 Rainfall vs Neumann above a Humus Layer

In both simulations in each model, the two continua behave in general terms in the same way and form similar saturation curves. Despite this, differences can be observed:

- Macropores at the high inflow simulation infiltrate more water in the Rainfall model than in the Humus Layer model, reaching a saturation degree of 0.2 instead of around 0.15 (day 3).
- On the other hand, water in macropores flows faster in the Humus Layer than in the Rainfall model (day 0.1).

8.3.3.2 Rainfall vs Neumann

Also in this couple of calculations, the final curves are almost identical. The time needed for reaching a steady state is also quite similar in both cases. Controlling the flux flowing over the fluxline set almost on the top of the domain in the two simulations, it is realised that for these values of inflow, water flows in both cases into the matrix. This means that:

- The macropores in the Rainfall BC are not yet activated for such order of precipitation values. The level of rainfall beyond which also macropores are activated remains still open to investigation.
- The Rainfall model reacts successfully to the flow problem. As this is a modified Neumann condition, it was expected that in certain field of input values it should bring the same results as the Neumann BC.

9 Conclusions

Summarising the important points of this thesis, various aspects of the double-continuum model for a two-phase flow in MUFTE-UG were examined. Simulations were carried out first in an attempt to reach a steady state of water saturation in the flow domain. Different beta exchange values were tested in order to identify their possible influence on the flow and to choose the most appropriate for the study. Especially boundary conditions were investigated in several ways. Simulations were held, so that the function of Dirichlet and Neumann BC is understood via comparison of different cases. These cases were defined assuming varying values of boundary quantities, taking into account different scales of infiltration intensity. Finally, another boundary condition was implemented, the Rainfall BC, aiming at the forming of a condition representing a rainfall event. It was controlled through simulations with a wide range of input values and compared with the existing Neumann BC.

There are several conclusions to be drawn. First of all, macropores do influence the flow, by infiltrating fast the water obtained from the exchange with the matrix. Second, the macroscopic heterogeneity of the ground, meaning for instance stratified formations, is also responsible for enhancing the role of macropores, in phenomena such as bypassing. Furthermore, boundary conditions function in different ways regarding the behaviour of the boundaries in the infiltration process. Last, the implemented Rainfall BC does correspond to realistic conditions and produces expected results.

However, there are still weak points in simulating infiltration in a fully satisfactory manner. Most important is the fact that values for quantities such as the beta exchange parameters and the length of interfaces adopted, are more or less arbitrary. Experiments should therefore be held in the laboratory, in order for a trustworthy database to be created and to verify the results extracted from software applications. Apart from that, further development of the Rainfall BC is needed. It is very significant that the rainfall intensity causing activation of macropores is examined through more simulations, which would exceed the aims and extends of the present thesis. Various parts of the implemented condition could as well be improved. One of them is the implementation of a more realistic rainfall event, e.g. through a time series, or of a long-term precipitation

input, e.g. generated stochastically. Regarding the above, further steps are yet to be made so that MUFTE-UG can finally be used on real field.

Bibliography

- Aitken, P., & B. L. Jones, *C in 21 Tagen*, Markt+Technik, 2000.
- Bear, J., *Dynamics of Fluids in Porous Media*, Dover, 1988.
- Beven, K., & P. Germann, Macropores and water flow in soils, *Water Resources Research*, 18, 1311–1325, 1982.
- Cirpka, O., Ausbreitungs- und Transportvorgänge in Strömungen i: Strömungen in natürlichen Hydrosystemen, lecture Notes for Stuttgart University.
- Edwards, W., L. Norton, & C. Redmond, Characterising macropores that affect infiltration into nontilled soils, *Soil Science Society of America Journal*, 52, 483–487, 1988.
- Gerke, H., & M. van Genuchten, A dual porosity model for simulating the preferential movement of water and solutes in structured porous media, *Water Resources*, 29, 305–319, 1993.
- Germer, K., L. Stadler, R. Hinkelmann, & J. Braun, Studies on infiltration processes in a soil column with a single macropore, EGU General Assembly, Vienna, 13-18 April 2008, 2008.
- Gisi, U., R. Schenker, R. Schulin, F. Stadelmann, & H. Sticher, *Bodenökologie*, Thieme, 1997.
- Hartge, K. H., & R. Horn, *Einführung in die Bodenphysik*, Enke, 1999.
- Helmig, R., *Multiphase Flow and Transport Processes in the Subsurface*, Springer, 1997.
- Helmig, R., Folien zur Vorlesung über Finite Methoden, 2004, lehrstuhl für Hydromechanik und Hydrosystemmodellierung, Institut für Wasserbau, Universität Stuttgart.
- Hinkelmann, R., *Efficient Numerical Methods and Information- Processing Techniques for Modeling Hydro- and Environmental Systems*, Springer, 2005.

- Jarvis, N. J., A review of non-equilibrium water flow and solute transport in soil macropores: principles, controlling factors and consequences for water quality, *European Journal of Soil Science*, 58, 523–546, 2007.
- Kavvas, M., *Soil Mechanics*, National Technical University of Athens, 2005.
- Kavvas, M., *Environmental Geotechnics*, National Technical University of Athens, 2007.
- Kiusalaas, J., *Numerical Methods in Engineering with Python*, Cambridge University Press, 2005.
- Lindenmaier, F., Hydrology of a large unstable hillslope at ebnet, vorarlberg identifying dominating processes and structures, Ph.D. thesis, Mathematisch-Naturwissenschaftliche Fakultät der Universität Potsdam, 2007.
- Mieth, S., Kopplung von numerischen Modellierungssystemen unter Verwendung von OpenMI and XML-RPC, Master's thesis, TU Berlin, Institut für Bauingenieurwesen, Fachgebiet Wasserwirtschaft und Hydrosystemmodellierung, 2008.
- Neunhäuserer, L., Diskretisierungsansätze zur Modellierung von Strömungs- und Transportprozessen in geklüftet-porösen Medien, Ph.D. thesis, Universität Stuttgart, Institut für Wasserbau, 2003.
- Paul, M., & H. Class, Folien zur Hydroinformatik, 2004, Lehrstuhl für Hydromechanik und Hydrosystemmodellierung, Institut für Wasserbau, Universität Stuttgart.
- Shipitalo, M., & K. R. Butt, Occupancy and geometrical properties of lumbricus terrestris l. burrows affecting infiltration, *Pedobiologia*, 43, 782–794, 1999.
- Simunek, J., N. Jarvis, M. van Genuchten, & A. Gärdenäs, Review and comparison of models for describing non-equilibrium and preferential flow and transport in the vadose zone, *Journal of Hydrology*, 272, 14–35, 2002.
- Stadler, L., J. Mayer, & R. Hinkelmann, Modellierung der Wasserinfiltration über Makroporen- vom Labor auf den Berghang, in *Forum Umwelttechnik und Wasserbau, Band 2*, Innsbruck University Press, 2008.
- Stadler, L., R. Hinkelmann, & E. Zehe, Two-phase flow simulation of water infiltration into layered natural slopes inducing soil deformation, in *Landslide Processes, From Geomorphologic Mapping to Dynamic Modelling*, Strassburg, France, 6–7 February 2009, 2009.